

Nuclear Magnetic Resonance in Uranium Hydride and Deuteride†

J. GRUNZWEIG-GENOSSAR, MOSHE KUZNIETZ,* AND BALFOUR MEEROVICI‡
Department of Physics, Technion-Israel Institute of Technology, Haifa, Israel
 (Received 22 August 1969)

β -uranium-hydride and β -uranium-deuteride are ferromagnetic with Curie temperatures of 182 and 178°K, respectively. Nuclear-magnetic-resonance studies of the proton in β -UH₃, and of the deuteron in β -UD₃, were made in the paramagnetic state of these compounds. The measured hydrogen Knight shifts (K) in β -UH₃ and β -UD₃ are given by $K = (0.40 \pm 0.03)\chi_M$, where χ_M is the molar susceptibility. The second moments are determined as $M_2 = (24 \pm 2) + (45 \pm 3) \times 10^{-4} h^2$ Oe² in β -UH₃, and $M_2 = (56.4 \pm 1.5) + (48.5 \pm 3) \times 10^{-4} h^2$ Oe² in β -UD₃, where $h = H_0/(T - \theta)$, θ being the appropriate paramagnetic Curie temperature. Analysis of the linewidth, line shape, and second moment showed that there are three line-broadening mechanisms (four in the deuteride): internuclear dipolar broadening, the (classical) dipolar field of the 5f electrons on the uranium ions, and an effect due to the use of powder samples (in the deuteride, a quadrupolar interaction is also present, with $|e^2qQ/h| = 14.5 \pm 0.5$ kHz). The line shapes, due to the simultaneous presence of several broadening mechanisms, are discussed in some detail. The 5f electrons are shown to be localized and do not form a band. The ferromagnetic interaction was analyzed using a simple Ruderman-Kittel-Kasuya-Yosida model, from which it is deduced that the coupling constant $\Gamma \sim 20$ eV Å³, $m^*/m_e \sim 3$, and the concentration of conduction electrons is about 2.5 per uranium ion. The Knight shift and quadrupole shielding were calculated, assuming the presence of a high-density interacting electron gas. At temperatures above 370°K, line narrowing was observed, from which the activation energy for hydrogen diffusion was obtained as $E = 8.4 \pm 0.9$ kcal/mole for the hydride and 8.9 ± 0.9 kcal/mole for the deuteride. It was concluded, on the basis of the pre-exponential term τ_0 of the correlation time τ_c , that diffusion takes place by a vacancy mechanism, and that the higher values of τ_0 and τ_c for the deuterium are mainly due to a difference in the relaxation mechanism. The valency of the uranium ions present has not been definitely established; they are either U³⁺ or U⁴⁺, probably the latter.

I. INTRODUCTION

ACTINIDES and their compounds, because of their incomplete 5f shell, exhibit interesting electrical and magnetic properties similar to those of the rare-earth elements. This field of research has been active since the last war, stimulated by the interest and availability of new actinide elements, although most work has been carried out on uranium and its compounds. This paper describes nuclear-magnetic-resonance (NMR) measurements on β -uranium-hydride and discusses its properties, using a model similar to that employed recently by us in a review of some uranium compounds.¹ Although its crystal structure is comparatively complicated, uranium hydride was chosen, since we hoped that at least one of its constituents, the hydrogen, would lend itself to analysis. A variety of other experimental data is also available, since β -UH₃ has been the subject of extensive research due to its potential applications in nuclear engineering.

β -uranium-hydride and β -uranium-deuteride are ferromagnetic below 182 and 178°K,²⁻⁶ respectively.

† Based on thesis dissertations submitted to the Senate of the Technion-Israel Institute of Technology, Haifa, as partial fulfillment of the requirements for D.Sc. degree (by M. K.) and M.Sc. degree (by B. M.).

* Present address: Solid State Science Division, Argonne National Laboratory, Argonne, Ill. 60439.

‡ Present address: Universidad Nacional de Ingenieria (Facultad de Ciencias Fisicas y Matematicas), Lima, Peru.

¹ J. Grunzweig-Genossar, M. Kuznietz, and F. Friedman, *Phys. Rev.* **173**, 562 (1968).

² W. Trzebiatowski, A. Sliwa, and B. Stalinski, *Roczniki Chem.* **26**, 111 (1952); **28**, 12 (1954).

³ D. M. Gruen, *J. Chem. Phys.* **23**, 1708 (1955); W. E. Henry and D. M. Gruen, *Phys. Rev.* **98**, 1200 (1955).

⁴ S. T. Lin and A. R. Kaufman, *Phys. Rev.* **102**, 640 (1956).

⁵ W. E. Henry, *Phys. Rev.* **109**, 1976 (1958).

⁶ A. I. Karchevskii, E. V. Artyushkov, and L. I. Kikoin, *Zh.*

This is a convenient system for investigating the NMR properties of the nuclei of nonmagnetic atoms in the paramagnetic state, since it contains a high concentration of such nuclei. Since its structure is stoichiometric,⁷ accurate numerical calculations can be made. In this paper, hydrogen (and hydride) usually refers both to H and D (or β -UH₃ and β -UD₃, respectively), whereas proton and deuteron are used if it is necessary to distinguish between the two isotopes.

The crystal structure of β -uranium-hydride was determined by Rundle,⁸ using x-ray and neutron diffraction techniques. The structure is cubic, with eight formula units per cell. The uranium atoms occupy the two types of sites of the β -W (A15) lattice (Fig. 1); two U_I atoms sit on a bcc lattice, while six U_{II} atoms complete the β -W structure. The 24 hydrogen atoms in the unit cell are all equivalent, forming a slightly deformed icosahedron around the U_I atoms. This, in turn, is surrounded by a similar larger icosahedron of the U_{II} atoms. Each U_{II} atom has also 12 equidistant hydrogen neighbors, but these are arranged less symmetrically than those around the U_I. All U_I-H and U_{II}-H distances are the same—2.30 Å. The shortest U-U (Table I) distances exceed the shortest distances in metallic uranium (2.76 Å in the α -uranium phase) and appreci-

Eksperim. i Teor. Fiz. **36**, 636 (1959) [English transl.: *Soviet Phys.—JETP* **9**, 442 (1959)]; A. I. Karchevskii, *ibid.* **36**, 638 (1959) [English transl.: *ibid.* **9**, 443 (1959)]; A. I. Karchevskii and E. M. Buryak, *Izv. Akad. Nauk SSSR, Ser. Fiz.* **25**, 1387 (1961); *Zh. Eksperim. i Teor. Fiz.* **42**, 375 (1962) [English transl.: *Soviet Phys.—JETP* **15**, 260 (1962)].

⁷ F. H. Spedding, A. S. Newton, J. C. Warf, O. Johnson, R. W. Nottorf, I. B. Johns, and A. H. Daane, *Nucleonics* **4**, 4 (1949).

⁸ R. E. Rundle, *J. Am. Chem. Soc.* **69**, 1719 (1947); **73**, 4172 (1951).

TABLE I. Properties of uranium hydrides and deuterides.

UX_3	Lattice constant (Å)	U-U (Å)	T_C (°K)	n_f (μ_B)	n_p (μ_B)	θ (°K)	References
β -UH ₃	6.631	3.310	182 181	1.18±0.03	2.44±0.04 2.59 2.79	176.1	2-8, 11-13, a
β -UD ₃	6.620	3.305	178.4 177.5	0.98±0.03 1.25 1.39	2.43	175.2	2, 5-8, 14-15
α -UH ₃	4.160	3.603	178	0.9	2.8	174	11-13
α -UD ₃	4.150	3.595	b,c c

^a E. J. Groat, J. T. Mason, and T. R. P. Gibb, *Rev. Sci. Instr.* **28**, 342 (1957).

^b R. Caillat, H. Coriou, and P. Pério, *Compt. Rend.* **237**, 812 (1953).

^c R. N. R. Mullford, R. H. Ellinger, and L. H. Zachariasen, *J. Am. Chem. Soc.* **76**, 297 (1954).

ably exceed the mean radius of the 5*f* electronic shell (~ 0.5 Å).

β -UH₃ was found⁷ to be a good conductor of electricity, although numerical values for the resistivity have not been published.⁹ This is in agreement with the recent results of measurements of the low-temperature specific heat of β -UH₃¹⁰; these showed a large term, linear in temperature, which, if interpreted by the simple Sommerfeld theory of electron specific heat, gives as the electron density at the Fermi level $n(E_F) = 12$ states/eV in the uranium atom.

The α allotropic form is metastable and difficult to prepare.¹¹⁻¹³ It changes irreversibly into the β form at temperatures above room temperature. The metal ions form a bcc lattice, with the hydrogens arranged on the faces of the cube, in the remaining sites of a β -W structure; this is the V₃Si lattice. Here, also, each uranium ion is surrounded by 12 hydrogens on the vertices of a slightly deformed icosahedron, and the U-H distances are the same as in the β phase. Thus, the local arrangements are very similar in the two allotropic forms.

The structural information and magnetic measurements²⁻⁶ are summarized in Table I and Fig. 1. Magnetization measurements^{4,5} give a value of $n_f = 1.18\mu_B$ for the ordered magnetic moment per uranium ion (in Bohr magnetons).

In neutron-diffraction studies,^{14,15} a value of $n_f = 1.39\mu_B$ was obtained. There was no indication of any difference between the moments of the U_I and U_{II} sites,

⁹ H. E. Flotow has measured the resistivity of a β -UH₃ sample of 90% of the theoretical density. The values (private communication) are $384 \pm 4 \mu\Omega\text{-cm}$ at 78°K and $700 \pm 15 \mu\Omega\text{-cm}$ at 193, 273, and 299°K. The temperature dependence is the one expected for magnetic materials.

¹⁰ H. E. Flotow and D. W. Osborne, *Phys. Rev.* **164**, 755 (1967).

¹¹ A. Sliwa and W. Trzebiatowski, *Bull. Acad. Polon. Sci., Ser. Sci. Chim.* **10**, 217 (1962).

¹² W. Spalhoff, *Z. Physik Chem. (Frankfurt)* **29**, 258 (1961).

¹³ E. Wicke and K. Otto, *Z. Physik Chem. (Frankfurt)* **31**, 222 (1962).

¹⁴ M. K. Wilkinson, C. G. Shull, and R. E. Rundle, *Phys. Rev.* **99**, 627 (1955); C. G. Shull and M. K. Wilkinson, Oak Ridge National Laboratory, Report No. ORNL-1879, 1955, pp. 24-27, (unpublished).

¹⁵ The neutron-diffraction study of β -UD₃ was recently repeated by G. P. Felcher, F. A. Smith, and M. Kuznietz at Argonne National Laboratory. The results confirm the results obtained in Ref. 14.

though they have different local symmetries. The magnetic properties of α -UH₃ were found¹¹ to be similar to those of β -UH₃, in spite of the different crystal structures and U-U spacings. The magnetic transition is also clearly shown by specific-heat measurements,¹⁶ where a peak was found at 170.7 and 167.6°K, which are close to the Curie temperatures of the hydride and deuteride, respectively.

Spalhoff¹² carried out Knight-shift and linewidth measurements on the proton NMR in the paramagnetic state of β -UH₃ and noted line narrowing at temperatures above 100°C. We report here our Knight-shift and linewidth measurements, which agree with those of Spalhoff, as well as determinations of the second moments and shapes of the NMR lines and their inter-

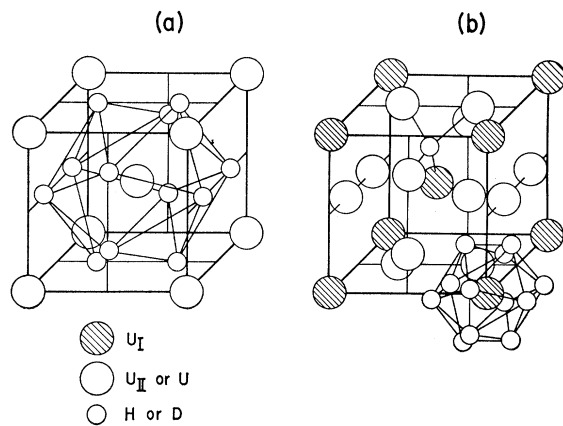


FIG. 1. The crystal structure of uranium hydrides. (a) For α -UH₃, the icosahedron formed by the 12 nearest hydrogens around a uranium site is shown; U: (0,0,0), $(\frac{1}{2}, \frac{1}{2}, \frac{1}{2})$; H: $\pm(\frac{1}{4}, 0, \frac{1}{2})$, $\pm(\frac{1}{2}, \frac{1}{4}, 0)$, $\pm(0, \frac{1}{2}, \frac{1}{4})$. (b) For β -UH₃, the tetrahedron of uranium ions around a hydrogen site are shown; U_I: (0,0,0), $(\frac{1}{2}, \frac{1}{2}, \frac{1}{2})$; U_{II}: $\pm(\frac{1}{4}, 0, \frac{1}{2})$, $\pm(\frac{1}{2}, \frac{1}{4}, 0)$, $\pm(0, \frac{1}{2}, \frac{1}{4})$; H: $\pm(0, u, \pm 2u)$, $\pm(\frac{1}{2}, \frac{1}{2} \pm 2u, \frac{1}{2} \pm u)$ cyclic. $u = 0.155$.

¹⁶ H. E. Flotow, H. R. Lohr, R. M. Abraham, and D. W. Osborne, *J. Am. Chem. Soc.* **81**, 3529 (1959); B. M. Abraham, D. W. Osborne, H. E. Flotow, and R. B. Marcus, *ibid.* **82**, 1064 (1960).

pretation. A preliminary report was published elsewhere.¹⁷

II. MEASUREMENTS

Powder samples of the hydride were obtained by the usual method of heating uranium lumps in hydrogen to 250°C, as described by Spedding *et al.*⁷ The uranium samples were of 99.7% purity and were obtained from Koch-Light Laboratories Ltd., Colnbrook, Bucks., England. The hydrogen was about 99.9% noninert gas, mixed with argon in a hydrogen-argon mixture. Deuterium gas (of 99% purity) was obtained from Bio Rad Labs., Calif. Samples were sealed in Pyrex capsules. The coil filling factor was about 0.6.

The powder particles were smaller than 2 μ . Using a minimal value for the electrical resistivity⁹ of 100 $\mu\Omega$ cm and a maximal frequency in the NMR measurements of 40 MHz, one obtains for the "skin depth" a value of 80 μ , which is well above the dimensions of the particles. Therefore, we did not expect any skin effects in our measurements.

Measurements were carried out both by the absorption (Pound-Knight) and induction (Bloch) methods for β -UH₃, but only by induction in β -UD₃, using constant radio frequencies and swept magnetic fields. An audio-frequency modulated magnetic field, not exceeding one-third of the linewidths, was used for recording the first derivatives of the NMR lines, with the help of a first-harmonic-tuned lock-in amplifier.

In the absorption method, we used a marginal regenerative oscillator of the Pound-Knight-Watkins type, produced by Nuclear Magnetics, Boston, Mass., with a frequency stability better than 1 in 10⁵. The sample coils were wound from pure copper wires or copper wires covered with Teflon, in order to eliminate any spurious proton signals. Calibration of the magnetic fields was performed, using water containing paramagnetic impurities (such as CoCl₂) in a separate coil. The signal-to-noise ratios were not too high, but increased with the rf level. Measurements were taken at room temperature and down to 207°K at fixed temperatures, using ice, dry ice, and freezing solutions as cooling materials.

In the induction method, we used a variable-frequency Varian unit (mode V-4210A) and the corresponding probes, in the range of 2-16 MHz. Adjustment of the system to the absorption mode was performed on the ¹⁹F NMR line in the surrounding non-hydrogen liquid 1,1,1-trifluoro,2,3,3-trichloropropene. The signal-to-noise ratios were better in this system. However, the low temperatures, achieved by passing of cooled nitrogen gas over the sample, were not as stable as those obtained using a freezing solution. Measurements were made at temperatures down to 202°K.

We were not able to saturate the proton NMR line at

room temperature with the highest rf field available (about 0.17 Oe). This gave an upper limit of 8 msec to the spin-lattice relaxation time T_1 . Indeed, in later measurements of T_1 , we found a room-temperature value of about 4 msec.

The deuteron line saturated at high rf field, and, as the signal-to-noise ratios were low, the parameters (H_1 , modulation amplitude, sweep rate, and time constant of the lock-in) had to be carefully selected. Unfortunately, in the case of the deuteride, the maximum obtainable temperature was limited to about 180°C by the Varian probe reaching its maximum permissible temperature.

We made sure that, in the recorded derivatives of the NMR lines, the areas above and below the zero axis were equal, so as to enable calculation of the second moments by numerical integration. The maximum error in determination of the second moment did not exceed 8%.

A. Knight-Shift Measurements

As reported earlier,^{12,17} the Knight shift K of the proton (deuteron) in the paramagnetic state of β -uranium-hydride is positive, i.e., the line recorded at constant frequency is shifted to lower fields with respect to the resonance field of protons in water. The experimental points obtained by Spalhoff,¹² together with our points, give the following temperature dependence for K :

$$1/K = (3.40 \pm 0.25)(T - \theta), \quad (1)$$

both for the proton and the deuteron in the temperature range up to 350°K. In the same range, the molar susceptibility χ_M is given in cgs (emu) units by^{2,3,6}

$$1/\chi_M = 1.25(T - \theta). \quad (2)$$

Thus,

$$K = (0.37 \pm 0.03)\chi_M, \quad (3)$$

which is shown in Fig. 2 for β -UD₃ (in Ref. 17 for β -UH₃).

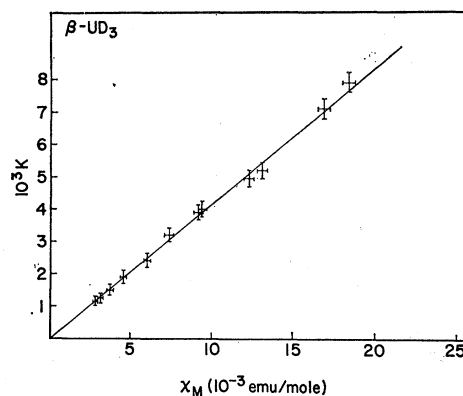


FIG. 2. Knight shift of β -uranium-deuteride as a function of the molar susceptibility.

¹⁷ J. Grunzweig and M. Kuznietz, in *Magnetic Resonance and Relaxation—Proceedings of the XIV Colloque Ampère, Ljubljana, 1966* (North-Holland Publishing Co., Amsterdam, 1967), p. 1131.

This result should be corrected for the effect of volume susceptibility and demagnetization of the particles in the powder grains, and for the shape of the sample as a whole. A partial discussion of this problem was made by Fert and Averbuch¹⁸ and by Ibers *et al.*¹⁹

In Appendix A, we show that the corrected Knight shift K is

$$K_r = (0.395 \pm 0.03) \chi_M. \quad (4)$$

The computed Knight shift, due to conduction electrons alone, is more than ten times smaller than the observed one (using simplifying assumptions that all conduction electrons are of the $1s$ type). It is probable that the Knight shift is caused mainly by interaction with the magnetic moments of the uranium ions via the conduction electrons [Ruderman-Kittel-Kasuya-Yosida (RKKY)-type mechanism]. This will be discussed at length in Sec. VII.

B. Linewidth and Second Moment

The measured linewidths, defined as the separation between the extrema of the derivatives of the lines, are summarized in Fig. 3. Since the hydride and deuteride differ in behavior, we shall discuss them separately.

In β - UH_3 , our cw and pulse measurements coincide with the cw measurements of Spalhoff¹² [see Figs. 3(a) and 3(b)]. We note a decrease in the linewidth, with rise of temperature, from 65 Oe at 200°K to 16 Oe at 295°K (in fields around 6000 Oe).

As the temperature is increased further, one finds that, from about 370°K, the line becomes narrower and the linewidth at 550°K is about 1.8 Oe. Spalhoff¹² attributed the decrease in linewidth to a "motional narrowing" caused by diffusion of hydrogen atoms.

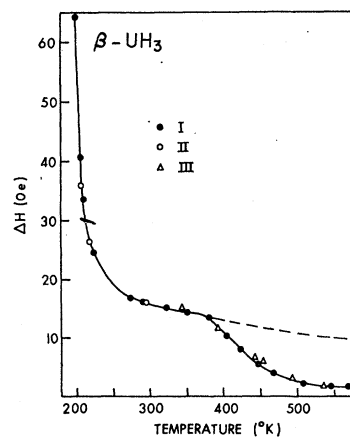
The linewidth is not proportional to susceptibility or magnetization. At room temperature, the line is almost symmetric. However, at lower temperatures, the line becomes asymmetric with a tail toward higher fields. We shall discuss the problem of the line shape in Sec. IV.

In β - UH_3 , the measured values of the second moment M_2 , with the error ranges, are plotted in Fig. 4 as a function of h^2 , where $h = [H_0/(T-\theta)]$, using for θ the value 183°K (approximately the Curie temperature of β - UH_3), which gives the best straight line. This can be written as

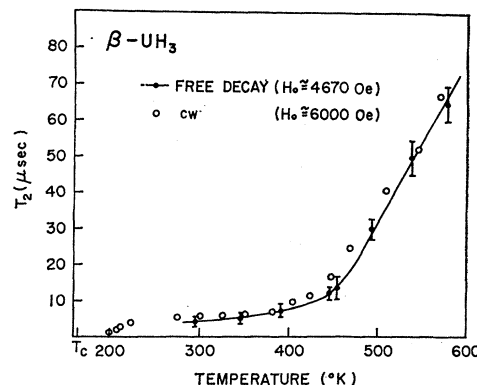
$$M_2 = (24 \pm 2) + (45 \pm 3) \times 10^{-4} h^2 \text{ Oe}^2, \quad (5a)$$

and it cuts the M_2 axis at $M_2(0) = (24 \pm 2) \text{ Oe}^2$. As $h = H_0/(T-183^\circ\text{K})$ is proportional to the magnetization in the paramagnetic state, the second moment is linear in the square of magnetization and the coefficient contains the various magnetization-dependent contributions, i.e., the contributions dependent on the

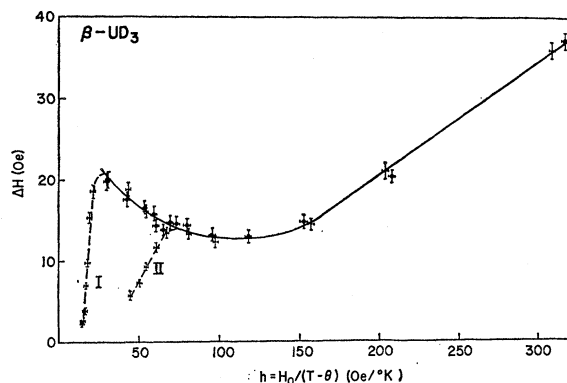
¹⁸ A. Fert and P. Averbuch, *J. Phys. (Paris)* **25**, 297 (1964).
¹⁹ J. A. Ibers, C. H. Holm, and C. R. Adams, *Phys. Rev.* **121**, 1620 (1961).



(a)



(b)



(c)

Fig. 3. (a) Linewidth of NMR lines in β - UH_3 in a field of ~ 6000 Oe as a function of temperature; (I) From Spalhoff (see Ref. 12); (II) cw measurements; (III) Pulsed NMR measurements. (b) The variation with temperature of the free decay-time constant T_2 of protons in β - UH_3 . Comparison is made with values deduced from cw linewidth assuming Gaussian lines (above room temperature). (c) Linewidth of NMR lines in β - UD_3 as function of $h = H_0/(T-\theta)$; (I) In $H_0 = 3800$ Oe; (II) In $H_0 = 12\,000$ Oe.

uranium ions. The intercept $M_2(0)$ should contain the internuclear interactions.

In β - UD_3 , the linewidth variation with temperature and magnetic field can be expressed over a wide range

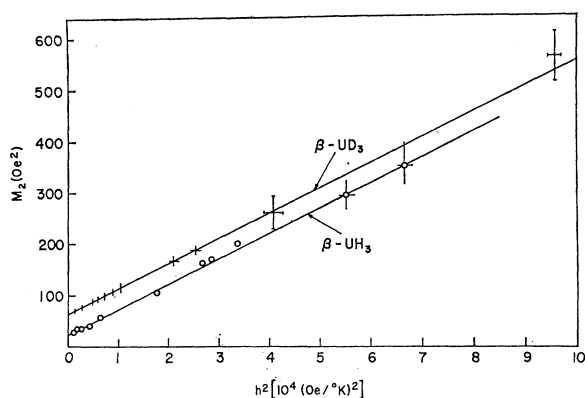


FIG. 4. Second moment of β - UH_3 and β - UD_3 as a function of h^2 .

as a function of a single variable, the "magnetization" $h = H_0/(T - \theta)$. This shows a minimum [Fig. 3(c)] at $h \approx 100 \text{ Oe}/^\circ\text{K}$. At sufficiently high temperatures, above about 370°K , we again observe narrowing due to diffusion of hydrogens. In this region, the linewidth cannot be described as function of magnetization only, and there is a slight variation from sample to sample. The latter effect seems to be due to the method of preparation, as impurities probably affect the vacancy concentrations and, hence, diffusion. This effect was not investigated further by us, and for diffusion measurements we used the results on our best samples.

The measured second moments are shown in Fig. 4. At temperatures under 370°K , all results fall on a straight line given by

$$M_2 = (56.4 \pm 1.5) + (48.5 \pm 3) \times 10^{-4} h^2 \text{ Oe}^2, \quad (5b)$$

which stretches over a very wide range of h^2 . The slope of the line equals that obtained in the case of the protons, within the experimental error. The zero intercept of the line equals the sum of the contributions of the internuclear dipolar and the quadrupolar second moments. It was used to determine the latter, and, hence, the quadrupole coupling in the deuteride.

III. LINEWIDTH AND SECOND MOMENT

There are several contributions to the NMR linewidths in paramagnetic materials. They arise from interactions between the investigated nucleus and its surroundings. Usually, each contribution appears as an additive term in the second moment. The various interactions are: (a) internuclear dipolar interactions ("Van Vleck" term); (b) electron-nuclear interactions; (c) quadrupole interactions (in the case of the deuteron only); (d) interactions arising from the powder structure.

The Hamiltonian of a nucleus in a paramagnetic material (neglecting the interaction between nuclear spins leading to the internuclear dipolar term) is given by

$$\mathcal{H} = -\gamma h \mathbf{I} \cdot (\mathbf{H}_0 + \mathbf{H}_L + \mathbf{H}_d) + \mathcal{H}_Q, \quad (6)$$

where \mathbf{H}_0 is the externally applied magnetic field, \mathbf{H}_L is the field due to the neighboring paramagnetic ions, and \mathbf{H}_d is the local field due to the demagnetization effect, especially important if the specimen consists of powder grains and is not a single crystal. \mathcal{H}_Q is the quadrupole interaction Hamiltonian.

A. Internuclear Interactions

The contribution of the interaction between the proton and the other nuclei was calculated by Van Vleck.^{20,21} The interaction with the ^{235}U nuclei ($<0.7\%$) can be neglected. Since there is only one type of hydrogen sites, the internuclear dipolar contribution to the second moment in a powder is given by

$$M_V = \frac{2}{5} \gamma^2 h^2 I(I+1) \sum_i r_{0i}^{-6} = L_N S_6, \quad (7)$$

where

$$S_6 = \sum_i (a/r_{0i})^6.$$

γ is the nuclear gyromagnetic ratio, I is its spin, a is the lattice constant, and r_{0i} is the distance between the investigated nucleus, located at the origin, and another hydrogen nucleus i . The sum S_6 depends on the crystal structure, and it converges rapidly. For protons $L_H = 4.183 \times 10^{-3}$, and for deuterons, $L_D = 2.380 \times 10^{-4} \text{ Oe}^2$. For the sum S_6 over 2729 nuclei, we find 5394, and integrating over the rest of the nuclei, we obtain the final value $S_6 = 5500$, which, in the case of protons, leads to $M_V = 23.0 \text{ Oe}^2$, in agreement with the experimental value $M_2(0)$ in Eq. (5a). For deuterons $M_V = 1.31 \text{ Oe}^2$.

In β - UH_3 at room temperature, we find, from Eq. (5a) for fields around 5600 Oe, that $M_2 = (34.5 \pm 2.5) \text{ Oe}^2$. The main contribution to this value is M_V , and that is the reason why we obtain almost symmetric lines at room temperature. The contribution of the internuclear term to the line shape is symmetric and can be represented approximately by a Gaussian function

$$F_V(H) = C \exp(-H^2/2M_V), \quad (8)$$

at least for the discussion of the low-temperature line shape.

The linewidth deduced from Eq. (8) is given approximately by $\Delta H = 2(M_V)^{1/2} \approx 10 \text{ Oe}$, and, for low values of h , the experimental linewidth will approach this value (in the absence of motional narrowing). In the vicinity of room temperature, Abragam-type functions²² approximate the observed line shapes more closely than Gaussians.

²⁰ J. H. Van Vleck, Phys. Rev. **74**, 1168 (1948).

²¹ A. Abragam, *Nuclear Magnetism* (Clarendon Press, Oxford, 1961).

²² Reference 21, p. 120.

B. Electron-Nuclear Interactions

There are several possible interactions between the investigated proton (deuteron) and the electrons in the crystal.

(i) A magnetic dipolar interaction between the average magnetic moments, localized on the uranium atoms, and the proton. This interaction was discussed by Kroon²³ and by Ibers *et al.*¹⁹ This is a long-range interaction which behaves as $\bar{\mu}r^{-3}$, where $\bar{\mu}$ is the average moment per magnetic ion (atom) in the paramagnetic state given by

$$\bar{\mu} = n_p^2 \mu_B^2 H_0 / [3k_B(T-\theta)] = \chi_M H_0 / N_A. \quad (9)$$

(ii) A magnetic dipolar interaction between the average magnetic moments localized on the hydrogen atoms and the proton. This interaction is of the same type as (i). However, we assume the absence of localized magnetic moments on the hydrogen atoms, as neutron diffraction studies in the ordered state could detect no moments localized on the hydrogen sites. Thus, even if there are small moments, their contribution is neglected with respect to that of the uranium ions.

(iii) A contact interaction between the uranium moments and the proton, which could be direct or indirect. Direct contact interaction is not effective, since the $5f$ shells are highly localized. Indirect interaction gives rise to the Knight shift via a RKKY-type mechanism. Its contribution to the second moment M_C exists whenever the ionic g tensor is anisotropic, and is given according to Ibers *et al.*¹⁹ as

$$M_C \sim (g_{11}^2 - g_{\perp}^2) A^2,$$

where A is the contact interaction constant, and g_{11} and g_{\perp} are the axial and azimuthal components of g , respectively. For the U_{II} sites, we expect an isotropic g tensor, since its site is of cubic symmetry. Since the magnetic properties of the U_{II} are the same as those of U_I , we expect that $g_{11} \sim g_{\perp}$, so that M_C is negligible.

To recalculate the paramagnetic contribution, item (i), we follow Kroon's method.²³ We assume that the investigated nucleus (at the origin) sees the fields produced by paramagnetic ions with moments $\bar{\mu}$, which are oriented parallel to the direction of the external magnetic field H_0 . We denote by \mathbf{r}_j (x, y, z) the radius vector between the origin and the j th atom with a moment $\bar{\mu}$, and ψ_j is the angle between \mathbf{r}_j and H_0 . The component of the local field H_L , parallel to $\bar{\mu}$ or H_0 , is

$$H_L = \sum_j \bar{\mu}_j r_j^{-3} (3 \cos^2 \psi_j - 1) = \sum_j (3z_j^2 - r_j^2) r_j^{-5}, \quad (10)$$

where the summation is over all the atoms with the same $\bar{\mu}$.

The field of such a dipole (or system of dipoles) at the origin transforms on rotation of the crystal, with respect to H_0 , as the components of a second-rank tensor. As

TABLE II. Lattice sums for the β -UH₃ lattice.

	H-U	H-H
S_{xx}	11.908 a^{-3}	20.822 a^{-3}
S_{yy}	6.813 a^{-3}	1.155 a^{-3}
S_{zz}	-18.721 a^{-3}	-21.937 a^{-3}
S_{xy}	-11.344 a^{-3}	28.008 a^{-3}
$S_{yz} = S_{zx}$	0	0
S_0	...	5500 a^{-6}

the field of the dipoles is small compared with H_0 , we consider only the component of H_L parallel to H_0 . In a given crystal orientation, we calculate the following sums over the dipole sites:

$$S_{ij} = \sum_k (3x_k^i x_k^j - \delta_{ij} r_k^2) r_k^{-5},$$

where x_k^i, x_k^j, x_k^l are the coordinates of the k th dipole. Table II shows the values calculated for the β -uranium-hydride lattice. If the crystal is now rotated so that the new orientation of the crystal coordinate axis is given by the polar angle with respect to the old ones, then the z component of H_L is given by

$$H_L(\theta, \phi) = 2 \left(\frac{4\pi}{5} \right)^2 \sum_{m=-2}^2 C_2^m Y_2^m(\theta, \phi). \quad (11)$$

In this equation, $H_{ij} = \bar{\mu} S_{ij} = h a_{ij}$, where the parameter $h = H_0 / (T - \theta)$ is proportional to the magnetization of the specimen. Y_2^m are spherical harmonics of second order and C_2^m are given by

$$\begin{aligned} C_2^0 &= \frac{1}{4} (5/\pi)^{1/2} H_{zz}, \\ C_2^{\pm 1} &= \mp (5/6\pi)^{1/2} \left(\frac{1}{2} \right) (H_{xz} \pm i H_{yz}), \\ C_2^{\pm 2} &= (5/6\pi)^{1/2} \left(\frac{1}{4} \right) (H_{xx} - H_{yy} \pm 2i H_{xy}), \end{aligned} \quad (12)$$

where $\bar{\mu}$ is the time average of the magnetic moment of the ionic dipole at each site. If there are several types of magnetic dipoles, $\bar{\mu}_r, \bar{\mu}_s, \bar{\mu}_t, \dots$, distributed over sites of type r, s , and t , the H_{ij} will contain sums over the different types of the appropriate lattice sums. The line shape of a randomly arranged powder specimen as function of the magnetic field H_0 depends on the distribution of nuclei over the local field H_L . This was computed by Bloembergen and Rowland,²⁴ and in more detail by Kroon,²³ and will be discussed in Sec. IV. The type of line shapes obtained^{23,24} is shown in Fig. 5(a). The second moment of such a line,

$$M_P = [(H_L - \bar{H}_L)^2]_{av},$$

is given by

$$M_P = (2/15) (\lambda_1^2 + \lambda_2^2 + \lambda_3^2), \quad (13)$$

where the λ 's are the roots of the matrix

$$\begin{vmatrix} H_{11} & H_{12} & H_{13} \\ H_{21} & H_{22} & H_{23} \\ H_{31} & H_{32} & H_{33} \end{vmatrix} = h \begin{vmatrix} a_{11} & a_{12} & a_{13} \\ a_{21} & a_{22} & a_{23} \\ a_{31} & a_{32} & a_{33} \end{vmatrix}. \quad (14)$$

²³ D. J. Kroon, Philips Res. Rept. 15, 501 (1960).

²⁴ N. Bloembergen and T. J. Rowland, Acta Met. 1, 731 (1953).

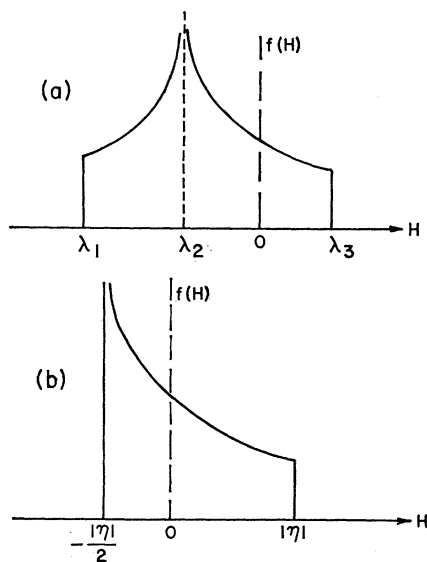


FIG. 5. Line shape arising from paramagnetic fields and powder structure. (a) Line shape (schematic) derived from Eq. (24); (b) line shape (schematic) derived from Eq. (26).

C. Quadrupole Interactions

The static quadrupole interaction term $3\mathcal{C}_Q$ shifts the energy levels. Ours is the case of high magnetic field,²⁵ where the quadrupole term is only a small perturbation as compared with the Zeeman term; hence, the magnetic field H_0 is the direction of quantization $0z'$. The quadrupole interaction, as given by the last term of Eq. (6), depends on the $z'z'$ component of the crystal gradient $eq = \partial^2 V / \partial z'^2 = V_0' = V_{zz}'$, calculated in the coordinate system with the $0z'$ parallel to H_0 .¹

To the first order of perturbations, the shift in the energy of the level m is given by

$$\Delta E_m = A[3m^2 - I(I+1)]V_0', \quad (15)$$

where $A = eQ/[4I(2I-1)]$. Hence, the frequency shift for the transition $m \leftrightarrow (m-1)$ is given by

$$\begin{aligned} \omega[m \leftrightarrow (m-1)] &= (\Delta E_m - \Delta E_{m-1})/\hbar \\ &= 3AV_0'(2m-1)/\hbar, \end{aligned} \quad (16)$$

which is equivalent to a local magnetic field

$$H' = 3AV_0'(2m-1)/(\gamma\hbar).$$

In the case of the deuteron, $I=1$; hence,

$$H' = \pm[3/(4\gamma\hbar)]V_0'eQ,$$

where the plus sign goes with the $m=1 \leftrightarrow 0$ transition and the negative sign goes with the $m=0 \leftrightarrow -1$ transition.

In order to calculate V_0' at the origin of coordinates,

²⁵ M. H. Cohen and F. Reif, in *Solid State Physics*, edited by F. Seitz and D. Turnbull (Academic Press Inc., New York, 1957), Vol. 5, pp. 321-438.

due to point charges Ze on sites $x_k, y_k,$ and z_k , we calculate lattice sums k_{ij} analogous to H_{ij} , where $\bar{\mu}$ is replaced by Ze .

Now, on rotation of the crystal, the dependence of V_0' (and, hence, of H') is given by an equation analogous to Eq. (11) with the $\bar{\mu}$'s replaced by Ze . If there are several types of charges, $Z_r e, Z_s e,$ and $Z_t e$ on sublattices r, s, t, \dots , the field gradient is the sum of the field gradients due to each type of charges.

As we measure linewidth, etc., in units of oersted, we introduce matrix elements $b_{ij} = \sum_r b_r(S_{ij})_r$, where $b_r = [3/(4\gamma\hbar)]e^2 Q Z_r$. The line shape and second moment of a powdered sample, in the case of quadrupole line broadening, are computed in a way analogous to that described in the paramagnetic case, Sec. III B, except that in the case of $I=1$ there are two transitions, giving rise to two sets of matrix parameters b_{ij} , differing in sign, and, hence, to two lines—mirror images of each other (see Fig. 6 for $h=0$).

A similar approach was used by Jones *et al.*²⁶ They analyzed the combined effect of an anisotropic Knight shift and a second-order quadrupole shift on the central NMR line of nuclei with $I \geq \frac{3}{2}$, and computed the positions of extrema and points of inflection.

D. Effect of Powder Structure

In paramagnetic powder samples, there are present additional line-broadening mechanisms, due to the magnetic field of the neighboring powder grains, and due to the variation of the demagnetization field over the randomly oriented nonspherical grains. This effect was estimated by Ibers *et al.*,¹⁹ Kroon,²³ and Drain.²⁷ Here, we shall follow Drain,²⁷ whose analysis seems the most complete. He showed that the first interaction brings about a symmetric line broadening, roughly Gaussian, while the second interaction gives rise to an asymmetric broadening which depends on their shape (assumed elliptical).

The demagnetization effect of each particle in the sample, and of the sample as a whole, must be taken into account.

The sample effects are connected with the average volume susceptibility of the sample χ_V' , while the particle effects are connected with material volume susceptibility χ_V . Since $\chi_V > \chi_V'$, the sample effect can be neglected, at least in the first approximation.

We assume that the sample consists of particles of similar shape, approximately spheroidal, where the ratio between the polar and azimuthal axes is m . The particles are assumed to be oriented randomly with respect to the external magnetic field. For a spheroid, there are two principal demagnetization factors, N_{11} and N_{11} , so that $N_{11} + 2N_{11} = 1$.

For a sphere, $N_{11} = N_{11} = \frac{1}{3}$, and, therefore, one can

²⁶ W. H. Jones, T. P. Graham, and R. G. Barnes, *Phys. Rev.* **132**, 1898 (1963).

²⁷ L. E. Drain, *Proc. Phys. Soc. (London)* **80**, 1380 (1962).

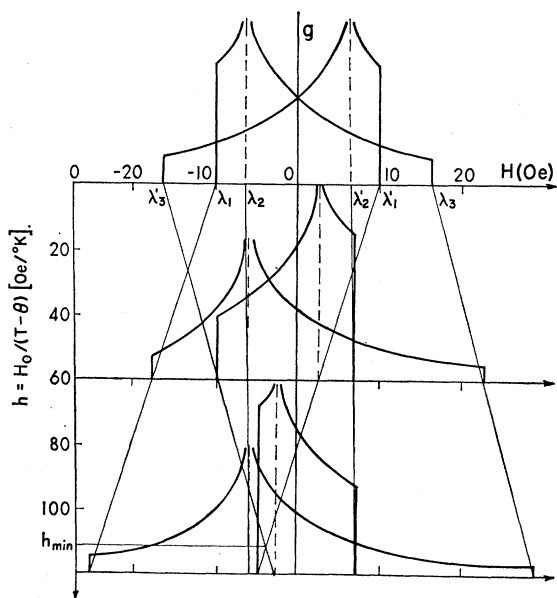


FIG. 6. The shapes of the lines of the deuterium doublet for several values of h , and the variation of λ 's, roots of Eq. (29), as a function of h .

describe the deviation of the demagnetization factors from $\frac{1}{3}$ by a factor η ,

$$N_{11} = +\frac{1}{3} + \eta \quad (17)$$

and

$$N_{12} = +\frac{1}{3} - \frac{1}{2}\eta.$$

For randomly oriented spheroids, the demagnetization fields are $4\pi M\nu$ ($-\eta \leq \nu \leq \frac{1}{2}\eta$) distributed around the value $4\pi M/3$, (where $M = \chi_\nu H_0$ is the magnetization per unit volume).

The distribution function $f(\nu)$ of these fields is finite for $|\nu| = |\eta|$, since the axial direction is unique, but there is an infinite number of equatorial directions ($|\nu| = \frac{1}{2}|\eta|$) for which the distribution function tends to infinity. The normalized distribution function is

$$f(\nu) = [3\eta(\eta - 2\nu)]^{-1/2}, \quad -\eta \leq \nu \leq \frac{1}{2}\eta \\ = 0, \quad \nu < -\eta, \frac{1}{2}\eta < \nu \quad (18)$$

for $\eta > 0$ and $\eta < 0$ with the condition (20b) for $\eta < 0$. The mean square deviation for $f(\nu)$ is

$$\bar{\nu}^2 = \int \nu^2 f(\nu) d\nu = \frac{1}{5}\eta^2. \quad (19)$$

Discussions of the demagnetization factors N_{11} , N_{12} for spheroids, and their relation to the ratio m were made by Chikazumi and by Morrish.²⁸ The actual calculation was carried out by Osborn and by Stoner.²⁹

²⁸ S. Chikazumi, *Physics of Magnetism* (John Wiley & Sons, Inc., New York, 1964); A. H. Morrish, *The Physical Principles of Magnetism* (John Wiley & Sons, Inc., New York, 1965).

²⁹ J. A. Osborn, *Phys. Rev.* **67**, 351 (1945); E. C. Stoner, *Phil. Mag.* **36**, 803 (1945).

The expressions for N_{11} are

for a prolate spheroid ($m > 1$)

$$N_{11} = (m^2 - 1)^{-1} [m(m^2 - 1)^{-1/2} \log(m + (m^2 - 1)^{1/2}) - 1], \quad (20a)$$

and for an oblate spheroid ($m < 1$)

$$N_{11} = (1 - m^2)^{-1} [1 - m(1 - m^2)^{-1/2} \arccos m]. \quad (20b)$$

If one supposes that the powder sample is built out of similar spheroids of a given m , one can use Eq. (18) to obtain the contribution M_D to the second moment

$$M_D = (4\pi M)^2 (\frac{1}{5}\eta^2) = (4\pi \chi_\nu H_0)^2 (\frac{1}{5}\eta^2), \quad (21)$$

which, for β -uranium-hydride, becomes

$$2300 \times (\frac{1}{5}\eta^2) \times 10^{-4} h^2.$$

In this expression, we have to assign a value for η . The assumption of prolate particles is confirmed by observation under the microscope, as well as by the work of Spedding *et al.*,⁷ who found that, in hydrogen under high pressure, the hydride grows as whiskers to a few millimeters in length. To get the best fit for the line shape using Eq. (18), we have to assume (see discussion below) that $m = 3$, so that

$$M_D = 20 \times 10^{-4} h^2 \text{ Oe}^2. \quad (22)$$

Combining the three contributions given by Eqs. (7), (13), and (22), we obtain the second moment of the proton and deuteron NMR lines in β -uranium-hydrides

$$M_2 = A + 44.5 \times 10^{-4} h^2 \text{ Oe}^2. \quad (23)$$

This relation is plotted in Fig. 4; it fits well the experimental curve of Eq. (5a), both for the hydride and for the deuteride.

IV. SHAPES OF NMR LINES

Each of the four interactions discussed in Sec. III makes its own contribution to the NMR line shape. The final result is obtained by convolution of functions, representing each of the contributing interactions. We have already mentioned that the internuclear (Van Vleck) contribution is symmetric and can be represented by a Gaussian curve given in Eq. (8). The line of the proton at room temperature is almost symmetric, since its main contribution is the internuclear dipolar contribution.

For the paramagnetic or quadrupolar line shape, we follow Kroon.²³ He defines the quantities $\Delta_{ij} = (\lambda_i - \lambda_j)$, the ratio $Q_r = \Delta_{32}/\Delta_{21}$, and obtains for the line shape the function

$$f_p(H) = 0, \quad H < \lambda_1 \\ = [(\lambda_3 - H)\Delta_{21}]^{-1/2} K [Q_r(H - \lambda_1)/(\lambda_3 - H)], \quad \lambda_1 \leq H \leq \lambda_2 \\ = [\Delta_{32}(H - \lambda_1)]^{-1/2} K \{ (\lambda_3 - H)/[(H - \lambda_1)Q_r] \}, \quad \lambda_2 \leq H \leq \lambda_3 \\ = 0, \quad \lambda_3 < H. \quad (24)$$

Here $K(k)$ is the complete elliptic integral defined as

$$K(k) = \int_0^1 \frac{dx}{(1-x^2)^{1/2}(1-k^2x^2)^{1/2}} = \int_0^{\pi/2} \frac{d\alpha}{(1-k^2 \sin^2 \alpha)^{1/2}}. \quad (25)$$

Discussion and values of this function are given by Milne-Thomson.³⁰

Such a paramagnetic line shape $f_P(H)$ is shown in Fig. 5(a) for β -UH₃ for $h=170$ Oe/°K. It is asymmetric, since $Q_r=0.7076$ is different from unity.

For the powder inhomogeneity line shape, we use the asymmetric function $f_D(H)$ as given by Eq. (18). In this case, $\eta < 0$ gives the correct line shape for β -UH₃ when combined with the contributions $f_V(H)$ and $f_P(H)$. $f_D(H)$ is given by

$$f_D(\xi) = \begin{cases} = 0, & \xi < -\frac{1}{2}|\xi_0| \\ = 4\pi\chi_V H_0 [3\xi_0(\xi_0 - 2\xi)]^{-1/2}, & -\frac{1}{2}|\xi_0| \leq \xi \leq |\xi_0| \\ = 0, & |\xi_0| < \xi \end{cases} \quad (26)$$

where ξ is $4\pi\chi_V H_0 \nu$ and ξ_0 is $4\pi\chi_V H_0 \eta$. The line shape of Eq. (26) is shown in Fig. 5(b). The parameter in $f_D(h)$, ξ_0 (or η), is connected with the shape factor of the particles m .

A. β -UH₃

To get the calculated shape of the NMR line, we have to perform a convolution of the three components, and obtain

$$G(H) = \int \int f_V(H-H''-H') f_P(H') f_D(H'') dH'' dH', \quad (27)$$

where $G(H)$ is the final computed absorption line shape (actually this is carried out for its derivative). The integration was performed by means of a computer (503 Elliott). There is good agreement between the calculated and experimental NMR lines, but only if we choose for m in $f_D(H)$ the value $m=3$ and, thus, $\eta = -0.22$. Figure 7 shows both the computed and observed line derivatives for 202°K and 3740 Oe. We get a good agreement, both for the second moment and the line shape, only if we choose the value $m=3$, although the two quantities are independent. The assumption of a cigar shape for the particles is quite reasonable, especially in view of the observations by Spedding *et al.*⁷ that, under pressure, the crystal habit of β -UH₃ is in the shape of needles. We also observed some of our powders under the microscope, under

³⁰ L. M. Milne-Thomson, in *Handbook of Mathematical Functions*, edited by M. Abramowitz and I. A. Stegun (U. S. Department of Commerce, National Bureau of Standards, Washington, D. C., 1964), Appl. Math. Ser. 55, Chap. 17, pp. 587-626.

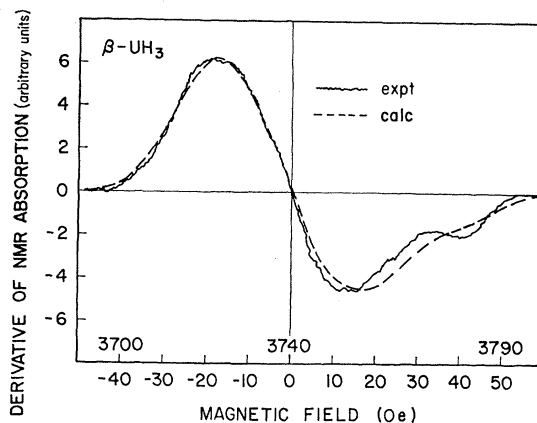


FIG. 7. Experimental and computed derivatives of NMR absorption lines of β -UH₃ in a field of $H_0=3740$ Oe and $T=202^\circ\text{K}$ ($h=170$ Oe/°K).

medium magnification, and the grain shape was in reasonable agreement with the above assumptions.

It should be noted that deviation from $m=3$ gives both a wrong line shape and a wrong value for M_2 . In effect, one obtains a completely different line shape when one omits the $f_D(H)$ contribution. The smoother calculated line in Fig. 7 is probably due to quite rough intervals in the numerical integration involved in Eq. (27).

B. β -UD₃

In the case of β -UD₃, all the four line-broadening mechanisms, including the quadrupole one, are present. However, the paramagnetic (Kroon) and quadrupole interactions are not independent, as both depend in a similar manner on the orientation of the given crystallite. Hence, the line shape obtained, due to interactions (b) and (c), is given by the procedure described in Sec. III B in the case of paramagnetic ions, except that the matrix elements in Eq. (14), etc., are now sums of paramagnetic and quadrupole terms:

$$\begin{bmatrix} ha_{11}+b_{11} & ha_{12}+b_{12} & ha_{13}+b_{13} \\ ha_{21}+b_{21} & ha_{22}+b_{22} & ha_{23}+b_{23} \\ ha_{31}+b_{31} & ha_{32}+b_{32} & ha_{33}+b_{33} \end{bmatrix} = ha \pm b. \quad (28)$$

The positive sign goes with the $m=1 \leftrightarrow 0$, and the negative sign with $m=0 \leftrightarrow -1$ transition. In uranium hydride, the zx and zy terms vanish. The roots of the two matrices are

$$\begin{aligned} \lambda_1 &= b_{33} + a_{33}h, & \lambda_1' &= -b_{33} + a_{33}h, \\ \lambda_{2,3} &= \frac{1}{2} \{ -(b_{33} + a_{33}h) \\ &\quad \pm [((a_{11} - a_{22})h + (b_{11} - b_{22}))^2 + 4(a_{12}h + b_{12})^2]^{1/2} \}, \\ \lambda_{2,3}' &= \frac{1}{2} \{ -(-b_{33} + a_{33}h) \\ &\quad \pm [((a_{11} - a_{22})h - (b_{11} - b_{22}))^2 + 4(a_{12}h - b_{12})^2]^{1/2} \}. \end{aligned} \quad (29)$$

The second moment of the two lines can be derived from Eq. (13) as

$$\begin{aligned} M_{PQ} &= (2/15)(\lambda_1^2 + \lambda_2^2 + \lambda_3^2 + \lambda_1'^2 + \lambda_2'^2 + \lambda_3'^2) \\ &= (2/15)(b_{11}^2 + b_{22}^2 + b_{33}^2 + 2b_{12}^2) \\ &\quad + (2/15)\hbar^2(a_{11}^2 + a_{22}^2 + a_{33}^2 + 2a_{12}^2). \end{aligned} \quad (30a)$$

Thus, it is equal to the sum of the paramagnetic and quadrupole partial lines second moments.

This second-moment contribution M_{PQ} should, therefore, be proportional to the square of the magnetization, with the same constant of proportionality as in $\beta\text{-UH}_3$. The measured second moment contains two additional terms (internuclear and powder structure), which, on convolution of the partial line shapes, will be added to M_{PQ} .

From Eq. (30a), the quadrupole contribution to the second moment can be written, referring to the principal axes x' , y' , and z' of the quadrupole field gradient as

$$\begin{aligned} M_Q &= (2/15)(b_{x'x'}^2 + b_{y'y'}^2 + b_{z'z'}^2) = \frac{1}{5}(1 + \frac{1}{3}\eta_Q^2)b_{z'z'}^2, \\ &= \frac{1}{5}(1 + \frac{1}{3}\eta_Q^2)(1/\gamma^2)[\frac{3}{4}e^2q'Q/\hbar]^2, \end{aligned} \quad (30b)$$

where $\eta_Q = (V_{x'x'} - V_{y'y'})/V_{z'z'}$ is the asymmetry parameter of the field gradient.²⁵

Figure 4 shows the observed second moment as a function of \hbar^2 . At low temperatures (below 370°K), M_2 is linear over a wide range of values of \hbar^2 , with a slope which agrees well with the calculated one for M_P and M_D and that measured in $\beta\text{-UH}_3$. Back extrapolation to $\hbar=0$ gives the sum of the internuclear dipolar and the quadrupole second-moment contributions $M_2(0) = M_V + M_Q = 56.4 \pm 1.5 \text{ Oe}^2$; hence, $M_Q = 55.1 \pm 1.5 \text{ Oe}^2$ (see Table III).

We calculated electric-field gradients (EFG) for different likely combinations of point charges on the uranium and hydrogen sites (see Table II), neglecting shielding. Apart from the term $\partial^2V/\partial x\partial y$, the uranium contributions are the major ones; hence, while the different point-charge combinations differ in the absolute magnitude of the matrix elements, their relative magnitudes do not change appreciably on going from one model to another, i.e., the anisotropy and orientation of the principal axis of the quadrupole-field-gradient tensor do not vary appreciably.

η_Q was calculated to be 0.1, assuming the field gradient to be due to appropriate point charges at lattice sites, and, as it is small, an error in η_Q will not affect appreciably the value of $V_{z'z'}$ derived from Eq. (30b). Thus, we obtain $|e^2q'Q/\hbar| = 14.5 \pm 0.5 \text{ kHz}$.

TABLE III. Contributions to the second moment (in Oe^2).

	M_V	M_Q	M_P	M_D
$\beta\text{-UH}_3$ calc	23	...	$2.46 \times 10^{-3}\hbar^2$	$2.0 \times 10^{-3}\hbar^2$
expt	24 ± 2	...	$(4.5 \pm 0.3) \times 10^{-3}\hbar^2$	
$\beta\text{-UD}_3$ calc	1.31	55.1 ^a	$2.48 \times 10^{-3}\hbar^2$	$2.0 \times 10^{-3}\hbar^2$
expt		56.4 ± 1.5	$(4.8 \pm 0.3) \times 10^{-3}\hbar^2$	

^a From the calculated M_V and the experimental $M_2(0)$.

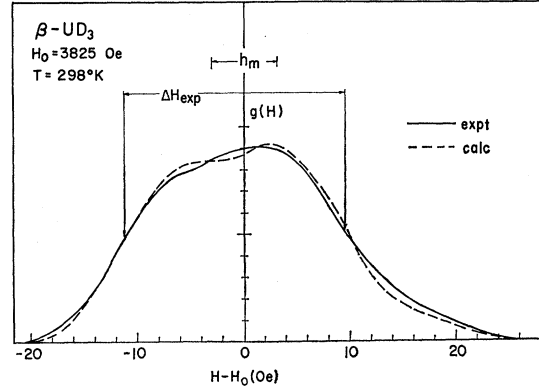


FIG. 8. Experimental and computed NMR absorption lines of $\beta\text{-UD}_3$ in a field of $H_0 = 3825 \text{ Oe}$ at $T = 298^\circ\text{K}$.

In order to reduce the computational work, we introduced the "average" relative quadrupole tensor elements, proportional to a scaling factor k , which was determined from the M_Q of the deuteride. This factor takes into account the shielding effects. We obtained (see above) the quadrupole coupling constant $e^2qQ/\hbar = (14.5 \pm 0.5) \text{ kHz}$, $\eta_Q = 0.1$, and used eventually

$$\begin{aligned} b_{11} &= 5.38 \text{ Oe}, \\ b_{22} &= 4.58 \text{ Oe}, \\ b_{33} &= -9.96 \text{ Oe}, \\ b_{12} &= -11.50 \text{ Oe}. \end{aligned}$$

The dependence of the roots λ as function of \hbar is shown schematically in Fig. 6, where the resulting line shapes are also shown, for several values of \hbar . One of the lines broadens with \hbar increasing, while the other narrows initially but later also begins to broaden. Thus, the resulting combined line first narrows and then broadens, as found in our measurements and shown in Fig. 3(c).

The recorded line shapes were compared with those computed by convolution of the partial line shapes due to paramagnetic and quadrupole partial line shapes described above, and with those due to internuclear interaction and powder (Drain) "interaction," as described previously in the case of $\beta\text{-UH}_3$. Figure 8 shows an example of such calculations; the agreement with the experiment is very satisfactory.

V. DIFFUSION OF H AND D IN URANIUM HYDRIDE AND DEUTERIDE

We measured the NMR linewidths and second moments of these compounds at temperatures above 350°K, where line narrowing was observed. This was attributed by Spalhoff¹² to hydrogen diffusion. We assume that the width and shape of the line are due to the interactions discussed in Sec. III. Their respective contributions to the low-temperature second moments are listed in Table III. In the case of the hydride, the internuclear dipolar contribution is dominant. In the

case of the deuteride, in low magnetic fields, the quadrupole interaction is most important; but as the magnetic field increases, the paramagnetic (Kroon) contribution also becomes important. At sufficiently high temperatures, the hydrogens begin to diffuse, and, when their jumping rate reaches T_2^{-1} (T_2 being the transverse relaxation time), the line begins to narrow. As the jumps are over atomic distances only, they cannot average out the Drain broadening effect. For the latter to average out also, the diffusion path must be of the order of the grain diameter³¹ (in our case about 1μ). As the line shape in the deuteride changes, we shall discuss the second moment. For our purpose, we use the reduced second moment

$$M_2' = (M_2)_{\text{exp}} - (M_2)_{\text{Drain}}, \quad (31)$$

which represents the mean square of the microscopic field fluctuation over atomic distances. The reduced second moment is plotted in Fig. 9. Initially, we shall discuss only the β -UH₃ and low-field β -UD₃ results. In the latter case, the two lines of the deuterium doublet are of approximately the same width and shape.

In our calculations, we have neglected the variation of the Kroon paramagnetic contribution over the temperature range where the measurements were carried out. This is a reasonable approximation, as these terms

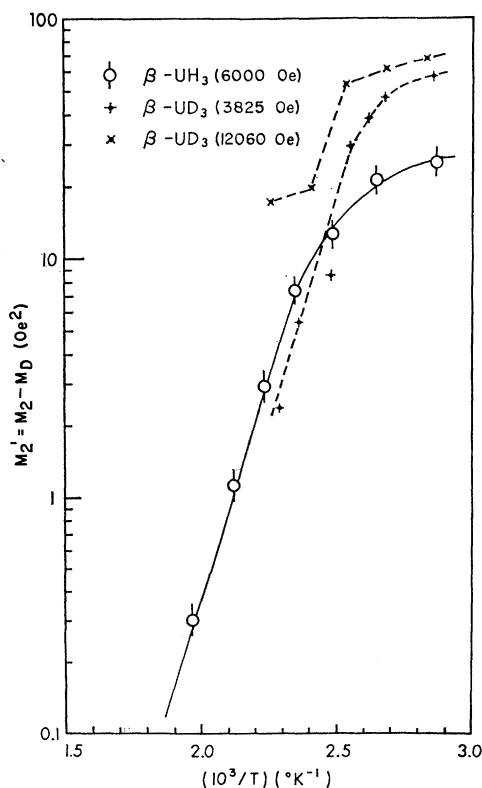


FIG. 9. The reduced second moment of β -uranium-hydrides as a function of the reciprocal of the temperature.

³¹ D. Zamir and R. M. Cotts, Phys. Rev. **134**, A666 (1964).

are small and change little over the temperature range used.

At sufficiently high temperature, we can put approximately²¹

$$1/T_2 \approx (\delta\omega_0)^2 \tau_c \quad \text{and} \quad \tau_c = \tau_0 \exp(E/RT),$$

hence, (32)

$$M_2'(T) \approx (\gamma M_2'^0 \tau_c)^2 = (\gamma M_2'^0 \tau_0)^2 \exp(+2E/RT),$$

where τ_c is the correlation time between fluctuations, $M_2'^0$ is the reduced-static low-temperature second moment (which does not include the Drain powder contribution), and E is the activation energy for diffusion (per mole). From Fig. 9, we find that, in both the hydride and the deuteride (low-field case), the activation energy obtained from the slope of the graph is the same within the limits of the experimental error

$$E(\beta\text{-UH}_3) = 8.4 \pm 0.9 \text{ kcal/mole} = 0.36 \pm 0.04 \text{ eV/atom},$$

$$E(\beta\text{-UD}_3) = 8.9 \pm 0.9 \text{ kcal/mole} = 0.39 \pm 0.04 \text{ eV/atom}.$$

This is a reasonable value for activation energy for diffusion in metal hydrides.³² Spalhoff's value of E for β -UH₃ ($E = 6.1$ kcal/mole) was obtained, neglecting the effect of the Drain term.

From Eq. (32), one finds that, at a given temperature, the ratio $r_{\text{expt}} = (\tau_c)_{\text{D}} / (\tau_c)_{\text{H}}$ is given by

$$r_{\text{expt}} = [M_2'(T)_{\text{D}} / M_2'(T)_{\text{H}}]^{1/2} \gamma_{\text{H}} M_2'^0_{\text{H}} / \gamma_{\text{D}} M_2'^0_{\text{D}} \quad (33)$$

$$= 2.2 \pm 0.3 \quad \text{at } 435^\circ\text{K},$$

while, from simple atomic-mass vibration-frequencies considerations, one would expect that $r_{\text{calc}} = \sqrt{2}$. Thus, the observed ratio r_{expt} is 1.6 ± 0.2 times that of the r_{calc} .

This is mainly an apparent discrepancy due to the method of measurement employed. Consider a deuteron: Its dominant line-broadening mechanism is the quadrupole interaction, which is localized; that is to say that every time the deuteron jumps to an adjoining site the change in the electric field gradient gives rise to a fluctuation in this Hamiltonian. Thus, τ_c equals the average stay on a given lattice site. However, in the case of a proton, the main line-broadening mechanism is the internuclear dipolar interaction; and, here, a relaxation can take place when the fluctuation arises due to the jumping either of the observed proton or any of its (near) neighbors.³³ The same reasoning is not applicable to the deuteride, since the neighboring deuterons (which are partially screened by the conduction electrons) contribute very little to the local electric field gradient and, hence, to the quadrupole interaction, compared with the uranium ions, which we assume to be stationary at these low temperatures.

In summing the contributions to the effective correlation time over the neighboring protons, one must

³² G. G. Libowitz, *Binary Metal Hydrides* (W. A. Benjamin, Inc., New York, 1965).

³³ M. Eisenstadt and A. G. Redfield, Phys. Rev. **132**, 640 (1963).

weigh their contributions by the square of the magnetic field contributed by each proton. Therefore, the effective correlation time at proton site i due to jumps by protons j is given by

$$\frac{1}{\tau_{\text{eff}}} = \frac{1}{\langle H_0'^2 \rangle} \left(\frac{1}{\tau_c} (\langle H_0'^2 \rangle + \sum_{j \neq i} \langle H_j'^2 \rangle) \right) = \frac{2}{\tau_c}, \quad (34)$$

for

$$\sum_{j \neq i} \langle H_j'^2 \rangle = \langle H_0'^2 \rangle = M_V.$$

The first term in the angular brackets of Eq. (34) represents the contribution due to jumps by the observed proton in the field of its stationary neighbors, while the other terms are due to jumps by its neighbors. Thus, $\tau_{\text{eff}} = \frac{1}{2}\tau_c$, which accounts, within the experimental error, for the difference between r_{calc} and r_{expt} obtained in Eq. (33). However, careful measurements of the diffusion of hydrogen isotopes in metals and nonmetals show values of r departing appreciably from the ratio of square root of their masses.³⁴

Line narrowing in uranium deuteride, in strong magnetic fields (Fig. 9), is a slightly more complicated process than that in the case of low field. As the paramagnetic (Kroon) local magnetic field is now quite appreciable, the two lines of the deuteron doublet have quite different widths and shapes (see Fig. 6). Hence, as the correlation time τ_c decreases with increase of temperature, the narrow line (large T_2) narrows first, and the wide line narrows appreciably later. This is shown schematically in Fig. 10. The slope of the high-temperature straight branch should be the same as that of the low-field graph. At $H = 12\,000$ Oe and 100°C , we calculated that the narrow line contributes 20% of the corrected second moment. The observed change in the second moment does not agree with this, since at the step the second moment is reduced (at $1/T = 2.3 \times 10^{-3} \text{ }^\circ\text{K}^{-1}$) by 70% of its low-temperature value, instead of as calculated above.

Flotow, Abraham, and co-workers calculated the Einstein vibration frequencies of the hydrogens in the crystal from specific heat and enthalpy of reaction of the hydrides.¹⁶ They obtained the following frequencies: In $\beta\text{-UH}_3$,

$$\nu_c = (810 | 940 | 1251) \text{ cm}^{-1} = (2.43 | 2.82 | 3.75) \times 10^{13} \text{ Hz};$$

in $\beta\text{-UD}_3$,

$$\nu_c = (572 | 664 | 885) \text{ cm}^{-1} = (1.72 | 1.99 | 2.66) \times 10^{13} \text{ Hz}.$$

Experiments on inelastic scattering of neutrons³⁵ were unable to resolve the expected frequencies of hydrogen vibrations. The measurements showed a broad band centered around 970 cm^{-1} with a width of 600 cm^{-1} in $\beta\text{-UH}_3$ (and around 710 cm^{-1} with a width of 400 cm^{-1}

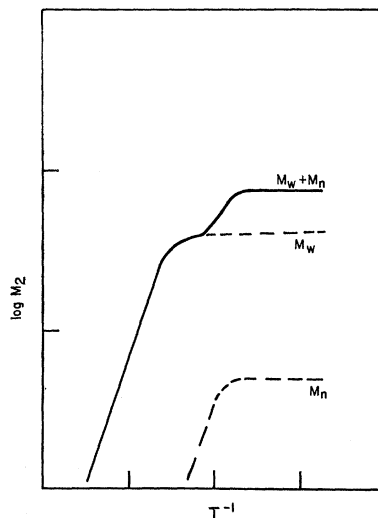


FIG. 10. Schematic changes of the second moment of the deuteron doublet as a function of T^{-1} in the region of motional narrowing. M_w is the second moment of the wide component of the doublet and M_n is the second moment of the narrow component.

in $\beta\text{-UD}_3$). The wide bands cover, in both cases, the three vibrational frequencies calculated from the specific-heat determinations.

From the diffusion measurements using Eq. (32), one finds that the pre-exponential terms give

$$\nu_0 = 1/\tau_0 = 4.5 \times 10^9 \text{ Hz, in } \beta\text{-UH}_3$$

and

$$\nu_0 = 1/\tau_0 = 3.7 \times 10^9 \text{ Hz, in } \beta\text{-UD}_3.$$

These frequencies are smaller by a factor of about 10^{-4} than the vibration frequencies of the hydrogen, as obtained from specific-heat and neutron-scattering experiments.

If diffusion takes place by a vacancy process, as found by Stalinski, Coogan, and Gutowsky³⁶ in the case of titanium hydride, then the concentration of vacancies determines the diffusion rate. Libowitz has discussed the problem of vacancies in uranium hydride.³⁷

From the consideration of the composition-pressure (s - p) diagram, he shows that the solubility of hydrogen in metallic uranium is very small (less than 10^{-3} at 500°C and 1 atmosphere pressure). The metal and the hydride coexist under well-defined decomposition pressures, which are an exponential function of temperature. Under this pressure, the hydride composition is slightly less than stoichiometric, UH_{s_2} ($s_2 < 3$), where s_2 corresponds to the right-hand knee on the s - p diagram and s_2 is given by

$$s_2(T) = 3 - C(0)e^{-\beta E(s)}, \quad \beta = 1/RT, \quad (35)$$

³⁶ B. Stalinski, C. K. Coogan, and H. S. Gutowsky, *J. Chem. Phys.* **33**, 933 (1960); **34**, 1191 (1961); C. K. Coogan and H. S. Gutowsky, *ibid.* **36**, 110 (1962).

³⁷ (a) G. G. Libowitz and T. R. P. Gibb, Jr., *J. Phys. Chem.* **61**, 793 (1957); (b) G. G. Libowitz, *J. Chem. Phys.* **27**, 514 (1957); (c) G. G. Libowitz, *J. Appl. Phys.* **33**, 399 (1962).

³⁴ P. M. S. Jones, *Nature* **213**, 689 (1967); A. D. LeClaire, *Phil. Mag.* **14**, 1271 (1966).

³⁵ J. J. Rush, H. E. Flotow, D. W. Connor, and C. L. Thaper, *J. Chem. Phys.* **45**, 3817 (1966).

where $C(0)$ is 0.6 and $E(s)$ is 6k cal/mole. On increasing pressure at constant temperature, s increases exponentially to $s_\infty(T)$ (< 3). Libowitz suggests [Ref. 37(b)] that $(1 - \frac{1}{3}s_\infty)$ is the fraction of sites inaccessible to hydrogen due to the presence of Schottky defects in the uranium lattice. He also shows that the s - p diagrams can be interpreted on the assumption that the energy for the creation of vacancies in β -UH₃ is 69.3 kcal/mole and that there is an attractive interaction energy between vacancy pairs E_{vv} of 4.4 kcal/mole. The crystal structure of uranium hydride shows that hydrogen sites are actually arranged in pairs, and an appreciable interaction between pairs of vacancies occupying such neighboring sites seems plausible.

If diffusion takes place by vacancy mechanism at the dissociation pressure of the hydride, the jumping rate should be proportional to the available fraction of hydrogen sites occupied by vacancies; thus,

$$\nu(T) = z\nu_0 e^{-\beta E_b} \frac{1}{3} [s_\infty(T) - s_2(T)] \\ = \frac{1}{3} z\nu_0 C(0) e^{-\beta [E_b + E(s)]}, \quad (36)$$

that is, the observed activation energy is the sum of the barrier height E_b and the vacancy-formation energy $E(s)$, and z is the number of neighboring hydrogen sites ($= 3$). Our experiments were performed on samples sealed off under vacuum while the hydride was at room temperature. Then, on heating, when the equilibrium concentration of hydrogen decreases as hydrogen is liberated, the pressure in the container increases rapidly, and the vacancy concentration in the hydride increases at a much slower rate than it does in the hydride under its dissociation pressure. The details of the temperature dependence of the pressure of formation and decomposition of uranium hydride are rather more complicated because of hysteresis at temperatures between 200 and 450°C, but apparently this hysteresis vanishes at lower and higher temperatures.¹³ In our experiment, the accessible-vacancies concentration changes with temperature, though at a much reduced rate compared with an "open" system. The density of vacancies as a function of temperature of our samples could be calculated from the s - p data of Libowitz and Gibb, the known mass of material, and the volume of the container. However, at 450°C, their data for the high- s end of the diagram already show great scatter. The extrapolation to lower temperatures, where our experiments were carried out, is therefore doubtful, and we have preferred to analyze our results on the assumption of a constant-vacancy concentration. Thus, our results overestimate the activation energy for hydrogen jumping, as the experimental results contain a contribution connected with increase of vacancy concentration with temperature.

We estimate from the s - p curves using Eq. (35) that the concentration of vacancies in the hydride, on sealing off, was about $C_v = 10^{-5}$. This, though rather small, seems to give the right order of magnitude for the pre-

exponential factor of the jumping frequency, which now becomes, for the hydride,

$$\nu_0 = z\nu_0 C_v = 3 \times 3 \times 10^{13} \times 10^{-5} \simeq 10^9 \text{ Hz.} \quad (37)$$

The available s - p data for β -UD₃ are not as extensive as those for β -UH₃ and, therefore, it is difficult to determine the concentration of vacancies in the deuteride material. The dissociation pressure is given by^{7,13}

$$\log_{10} p = -(A/T) + B, \quad (38)$$

where p is in mm Hg, A is 4500 for both compounds, and B is 9.20 for the hydride and 9.40 for the deuteride.

Thus, the vacancy concentration in the deuteride is probably slightly higher than in the hydride at a given temperature and pressure. Assuming that for a given dissociation pressure the s - p curves in the two compounds coincide, the vacancy concentration in the deuteride is about 14% higher than in the hydride. However, in our calculation we have neglected this effect.

We also considered the possibility that hydrogen diffusion takes place not by "jumping over a barrier" but by a tunneling process,³⁸ either from the ground state or from an excited level. We used a double-well model, where the potential barrier becomes thinner toward the top. The hydrogens, when thermally excited to higher vibration levels, encounter a barrier thinner than in the ground state, and can thus, tunnel through it. Such a model has been described repeatedly in the literature. That the diffusion activation energy is the same in the hydride and the deuteride can be explained by arguing that, although the vibration energy level spacings for the two compounds are different, the activation energy is the same, as it is determined by the height where the barrier thicknesses are similar. The comparison of the diffusion activation energy with the hydrogen vibration frequencies show that the excited levels, where tunneling apparently takes place, correspond to high-vibrational quantum numbers ($n \sim 20$). Since the lattice constant in the deuteride is slightly smaller, the barrier thickness should be reduced compared with that in the hydride. However, such a model could not account for the nearly doubling of tunneling frequency on going from the hydride to the deuteride, unless very artificial assumptions are made. It seems that in other metal hydrides, also, the jump model for hydrogen diffusion is applicable in preference to the tunneling model.

VI. MAGNETIC INTERACTIONS

In discussing the properties of β -uranium-hydride, we shall assume that its magnetic properties are due

³⁸ T. P. Das, J. Chem. Phys. **27**, 763 (1957); J. A. Sussmann, Physik Kondensierten Materie **2**, 146 (1964); J. A. Sussmann, in *Electron Magnetic Resonance and Solid Dielectrics—Proceedings of the Colloque Ampère, Bordeaux, 1963* (North-Holland Publishing Co., Amsterdam, 1964), p. 562.

mainly to localized $5f$ electrons, which interact through the conduction electrons; we shall stress the similarity in the magnetic properties of the α and β allotropic forms. The uranium ions are the carriers of the magnetic moments. The site symmetry of the uranium ions is derived from the icosahedral point group. In the case of α -UH₃ and of U_I in β -UH₃, the 12 hydrogens, instead of forming an icosahedron with equilateral triangles, form one with isosceles faces, the bases of which are ~ 2.05 Å, and their sides ~ 2.52 Å. At the U_{II} sites, the distortion of the surrounding icosahedron is quite appreciable, the hydrogens being grouped in threes. The local-site symmetry in α hydride and of U_I is T_h , and that of U_{II} is D_{2d} . The exact calculations of the magnetic properties of such cations in the crystalline field of their neighboring ions is hardly feasible, since the values of the numerous crystalline field parameters, on the low-symmetry sites, are difficult to determine, unless detailed data, e.g., optical, are available. We shall now try to use arguments similar to those employed in dealing with uranium compounds with rock salt structure.¹

We assume that the ground state of uranium ions is determined with reasonable approximation by the Russell-Saunders coupling and Hund's rules. Uranium appears in its compounds with a valency varying between 2 and 6. Neutron diffraction measurements^{14,15} at 4°K showed that, in the ordered state, the magnetic moments on the U_I and U_{II} sites are the same. Hence, the ground state of the two types of ions, under the exchange interaction with their oriented neighbors and in the crystalline field of the two types of sites, must have the same moments. This may be coincidence, but, as there is also a close similarity in magnetic properties to α -UH₃, where all uranium ions are *identical*, we assume that in β -UH₃, too, all uranium sites contain ions of the same valency and similar ground level state. Let us consider the splitting of levels of the ground multiplet of the uranium ions under crystalline fields of gradually decreasing symmetry, in order to determine which ions have the same ground state on the α -UH₃ and on U_I and U_{II} sites of the β -UH₃. This is shown schematically in Fig. 11, determined from considerations of symmetry, for the ground multiplets of the three ions. The connection between the icosahedral and octahedral representations is not obvious, since the octahedral symmetry group is not a subgroup of the icosahedral.³⁹ It can be seen that only in the case of $5f^2(U^{4+})$ ion is there additional splitting of the ground multiplet on going from U_I to U_{II} sites. Thus, the criterion that the ground multiplets of ions on the U_I, U_{II}, and in α hydride must be the similar cannot defi-

³⁹ B. R. Judd, Proc. Roy. Soc. (London) **A241**, 122 (1957); B. R. Judd and E. Wong, J. Chem. Phys. **28**, 1097 (1958); A. G. McLellan, *ibid.* **34**, 1350 (1961); N. V. Cohan, Proc. Cambridge Phil. Soc. **54**, 28 (1958); G. F. Koster, J. O. Dimmock, R. G. Wheeler, and H. Statz, *Properties of the 32 Point Groups* (The MIT Press, Cambridge, Mass., 1963).

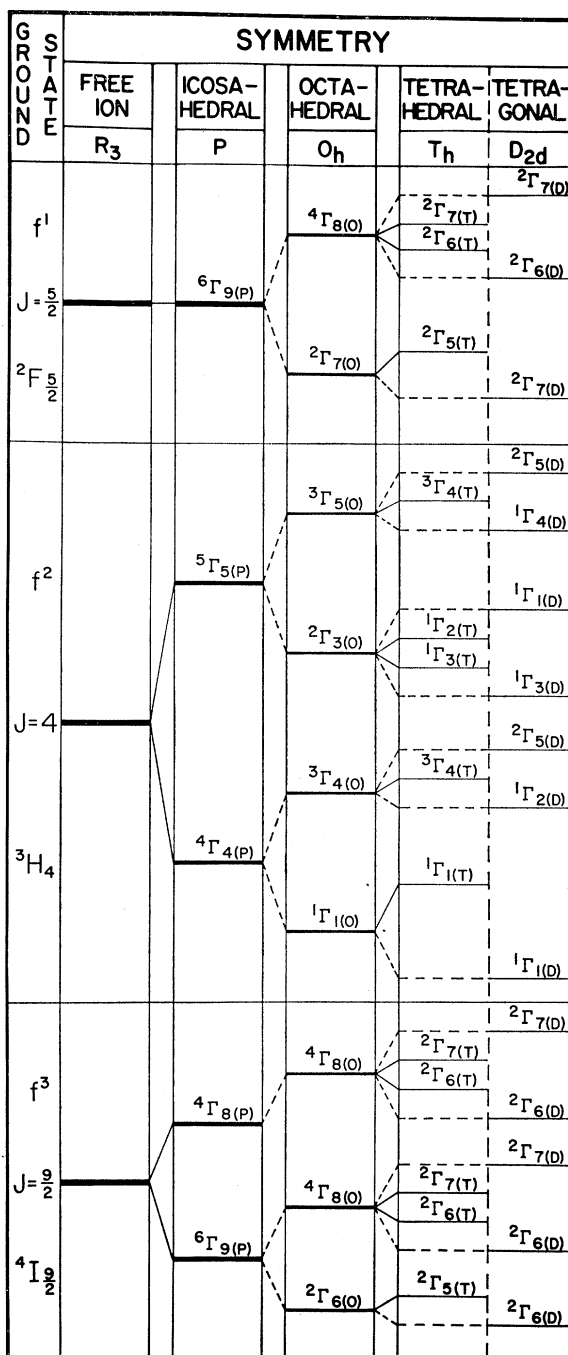


FIG. 11. Level splitting of the ground multiplet of the f^1 , f^2 , and f^3 ions in fields of decreasing symmetry (the drawing is schematic).

nately eliminate any of the three ions considered above. The additional splittings due to the reduction of the actual site symmetries from octahedral to tetrahedral or tetragonal, respectively, are presumably small (of the order of 10 cm^{-1}), and, as most susceptibility measurements were performed at sufficiently elevated temperatures (above T_c), these additional splittings would

hardly be detectable. Thus, the high-temperature susceptibility calculated on the assumption of octahedral site symmetry of the uranium ions should be sufficiently good approximation. This simplified case can be dealt with by the well-known methods of crystal field theory, which we think is applicable here. Of the remaining crystal field parameters, the first approximation will consider the case of "fourth-order term only" ($|x| \simeq 1$).^{1,40} Under such assumptions, one can calculate the magnetic susceptibility, and this can be compared with the experimental results. At temperatures well above the critical point, the molecular field theory of susceptibility in materials ordering at low temperatures can be safely employed. The observed paramagnetic moment per uranium ion $n_p = 2.6-2.79\mu_B$ in β -UH₃ cannot be easily reconciled with the values obtained from calculations for the three ions considered, even if one allows for an appreciable contribution to n_p from conduction electrons. It seems that the cube-coordinated f^2 ion is a possible candidate, though the n_p value here increases with temperature. Recent optical measurements on U⁴⁺ ions on D_{2d} sites by Richman *et al.*⁴¹ showed ground multiplet splitting which can be related to those on the octahedral-cube-coordinated ion. In their case, the ground state is the ${}^3\Gamma_{5(0)}$ which, under tetrahedral symmetry, remains a triplet, while under tetragonal symmetry splits into a singlet and doublet. Thus, in the ordered state at low temperature, U_I and U_{II} differ, which contradicts the neutron-diffraction results.

Consideration of the saturation magnetization at low temperature can also be employed in the search for the valency. The neutron-diffraction results give a value of $n_f = 1.39\mu_B$, which is slightly larger than the saturation magnetization results. The magnetization moment per ion, under the combined influence of the crystal field and the exchange interaction of the neighboring ions, can be calculated as described by Ebina and Tsuya,⁴² White and Andelin,⁴³ and by others.¹ Assume, arbitrarily, that the direction of the Weiss field is parallel to a fourfold axis of an octahedral site. Experience shows that, when switching on a magnetic field, the magnetic moment of the ground level increases, hence, the values are the lower limits of the saturation magnetic moments. This consideration seems to exclude the f^3 ion. Thus, we conclude that the uranium ions are either in the f^1 or f^2 configuration, probably the latter. However, it is doubtful to what extent one can extrapolate from the octahedral case.

It seems likely that the interaction causing magnetic ordering is of the RKKY type.¹ Assuming there are

nearly free electrons, a spherical Fermi surface, and an exchange interaction between $5f$ and $7s$ electrons which is independent of $\mathbf{q} = \mathbf{k} - \mathbf{k}'$, the change in the conduction-electron momentum vector, we calculated the interaction terms between the uranium ions. There was a slight difference between the summation for a U_I and a U_{II} site. In Fig. 12, we plot the weighted average of the two as function of $2k_{Fa}$ or Z , where Z is the number of conduction electrons per UH₃ unit. We also calculated the interaction for the bcc lattice of the uraniums in α -UH₃. Taking into consideration the different numbers of ions per unit cell, the two graphs agree very closely up to $2k_{Fa} = 20$, where they begin to diverge. This, again, agrees with our assumption about the close similarity between the two allotropic forms of the hydride. The calculations show energy minima around $Z \sim 0.05$ (case A) and $Z \sim 2.5$ (case B) that are conditions which might lead to the appearance of ferromagnetic ordering at low temperatures. *A priori*, it is not clear which of the two minima describes the situation in uranium hydride, and, initially, we shall consider them both. To determine the coupling constant Γ and the effective mass of the conduction electrons m^* , one requires, apart from knowledge of T_C , information about the magnetic contribution to electrical resistivity.¹

As mentioned in Sec. I, the only available data on the electrical resistivity of β -UH₃ are the preliminary measurements by Flotow⁹ on compressed specimens. These measurements provide us with an upper limit of $\sim 500 \mu\Omega$ cm for the magnetic contribution ρ_m to the resistivity in the paramagnetic state. We assume that the actual value of ρ_m is in the range of 50–500 $\mu\Omega$ cm, well within the values of ρ_m for uranium compounds (with nonmetals) which order magnetically.¹ Figure 13 shows the dependence of $|\Gamma|$ and (m^*/m_e) on the value of ρ_m for both cases (A and B), under the assumptions of the three ionic configurations of the uranium ion. In case A, the above-mentioned range of ρ_m gives the values $0.2 < (m^*/m_e) < 0.6$ and $50 < |\Gamma| < 100 \text{ eV } \text{\AA}^3$. In case B, the values are $3 < (m^*/m_e) < 20$ and $6 < |\Gamma| < 30 \text{ eV } \text{\AA}^3$. The sign of the coupling constant has been determined from Knight-shift measurements (see Sec. VII): Γ is negative for case A and positive for case B. The values of $|\Gamma|$ and m^* obtained in case B seem reasonable and are similar to values deduced for UX compounds with NaCl-type structure¹ (X is an element of group VA or VIA). The intermediate values obtained for the U⁴⁺ configuration are $|\Gamma| \simeq 20 \text{ eV } \text{\AA}^3$ and $m^*/m_e \simeq 3$, and these are typical values for the other configurations, also. At the higher limit of ρ_m , the values in case A, $(m^*/m_e) \simeq 0.6$ and $|\Gamma| \simeq 50 \text{ eV } \text{\AA}^3$, although extreme, should not be disregarded. However, these values are less reasonable than in case B and differ appreciably from the UX values. In both cases, $|\Gamma|$ is higher than in lanthanide compounds, which was attributed to larger extent of the $5f$ electronic wave functions.¹ Γ is expected to have the same sign in β -UH₃ as in the UX compounds.

⁴⁰ R. V. Rahman and W. A. Runciman, *J. Phys. Chem. Solids* **27**, 1833 (1966).

⁴¹ I. Richman, P. Kisliuk, and E. Y. Wong, *Phys. Rev.* **155**, 262 (1967).

⁴² Y. Ebina and N. Tsuya, *Sci. Rept. Res. Inst. Tohoku Univ.* **12B**, 1 (1960); **12B**, 165 (1960); **12B**, 183 (1960); **15B**, 1 (1963); **15B**, 47 (1963); **15B**, 85 (1963).

⁴³ R. L. White and J. P. Andelin, *Phys. Rev.* **115**, 1435 (1959).

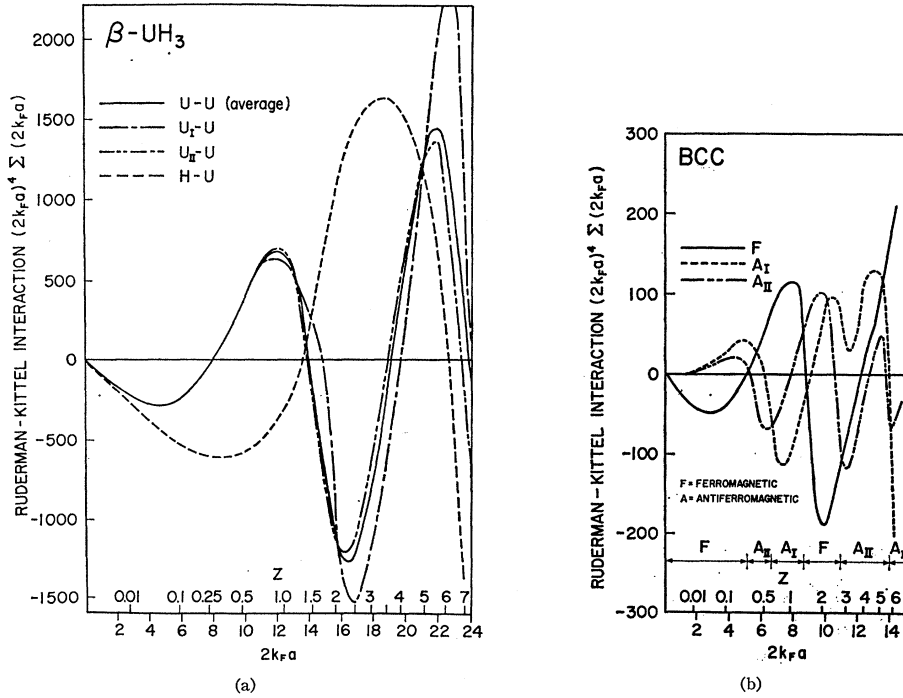


FIG. 12. (a) The RKKY interaction in $\beta\text{-UH}_3$ lattice. All inter-uranium interactions are practically the same. H-U interactions are used for Knight shift calculations. (b) The RKKY interaction in $\alpha\text{-UH}_3$ (bcc) lattice. Calculation for possible antiferromagnetic orderings are also included.

The lattice parameter, on going from the hydride to the deuteride, decreases by 0.011 \AA , and this is accompanied by a reduction of the Curie temperature by about 4°K . If one assumes that m^* and Γ remain constant, then the reduction of lattice constant should increase T_c , in contradiction with the experimental results. The ratio $\zeta = d[\log(T_c)]/d(\log V)$ in the uranium-hydride-uranium-deuteride system equals 4, in contradiction to the above conclusions. Experimental results on several rare-earth metals,⁴⁴ whose magnetic coupling mechanism is probably attributable also, to a RKKY interaction, show values of ζ within the range of $+0.7$ – $+2.5$, that is, of similar magnitude and sign as in the uranium compounds. It, therefore, seems that this does not contradict the assumption of a RKKY coupling, but probably changes of the lattice constant cause appreciable changes in Γ and/or in m^* . It should, however, be noted that more recent measurements on some lanthanide compounds⁴⁵ have found for ζ negative values of -2.2 in GdN and -5.5 in EuO.

VII. KNIGHT SHIFT

The Knight shift K_I in uranium hydride is presumably due to contact interaction between the proton spin \mathbf{I} at $\mathbf{R}=0$ and the spin of the conduction electron \mathbf{s} . If

the conduction electron has a wave-function amplitude $u(0)$ at the origin, the interaction is

$$\mathcal{H}_{\text{con}} = (8/3)\gamma_e\gamma_n h^2 \mathbf{I} \cdot \mathbf{s} u^2(0) = A(s)\mathbf{I} \cdot \mathbf{s}, \quad (39)$$

where γ_e and γ_n are the electronic and nuclear gyromagnetic ratios, respectively. The conduction electrons,

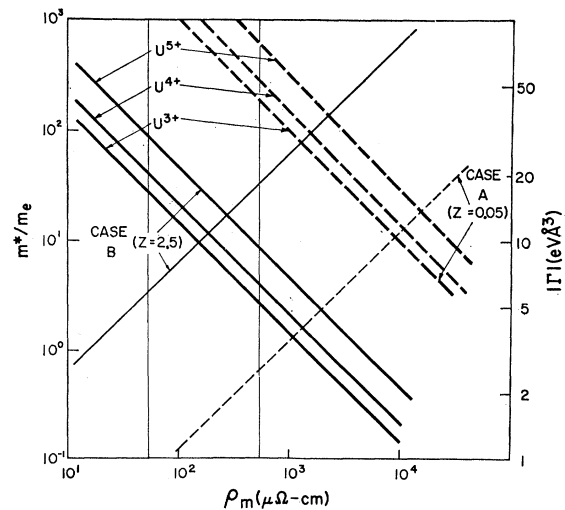


FIG. 13. The calculated $|\Gamma|$ (heavy lines) and m^*/m_e (light lines) as a function of the magnetic resistivity ρ_m for $\beta\text{-UH}_3$. The graph shows results for the three uranium ions both in case A ($Z \sim 0.05$, dashed lines) and in case B ($Z \sim 2.5$, solid lines). The vertical band corresponds to the range of presumed values of ρ_m .

⁴⁴ D. H. McWhan and A. L. Stevens, Phys. Rev. **139**, A682 (1965).

⁴⁵ D. B. McWhan, P. C. Souers, and G. Jura, Phys. Rev. **143**, 385 (1966), for EuO; D. B. McWhan, J. Chem. Phys. **44**, 3528 (1966), for GdN.

in turn, are polarized both by the external magnetic field H_0 and by interaction with the localized magnetic electrons in the $5f$ shells on the uranium ions. If one assumes simple RKKY coupling, as used in Sec. VI, one finds that the interaction between a $5f$ electron at \mathbf{R} of spin \mathbf{S} with the proton \mathbf{I} at the origin is

$$3\mathcal{C}_{IS} = -m^*\Gamma A(s)\Omega(2k_F)^4(8\pi\hbar^2)^{-1}F(2k_FR)\mathbf{I}\cdot\mathbf{S}, \quad (40)$$

where m^* is the effective mass, Ω is the normalizing volume for the conduction-electron wave functions, and $F(x)$ is the Ruderman-Kittel function. In a crystal, we sum F over all the paramagnetic ion sites \mathbf{R}_j , replace \mathbf{S} by its projection on \mathbf{J} (which is a good quantum number in this case), $\mathbf{S} = (g-1)\mathbf{J}$, and then replace \mathbf{J} by its time average as derived from the magnetic susceptibility χ_M of the uranium ions. We obtain, finally,⁴⁶⁻⁴⁸

$$K_I = -\frac{\chi_M m^* \Gamma (g-1) A(s) \Omega}{4\gamma_n g \mu_B N_A \hbar^3 a^4} P^I(2k_F a). \quad (41)$$

To this should be added the direct Knight shift, due to the interaction of the conduction electrons of the external magnetic field H_0 , but, here, this is negligible. The sum $P^I(2k_F a) = (2k_F a)^4 \sum_j F(2k_F R_j)$, which describes the dependence of the nucleus-paramagnetic-spin coupling as a function of k_F , is drawn in Fig. 12(a). The information about the Knight shift enables one to determine the sign of Γ if $P(x)$ is known. For case A (Sec. VI), P^I is about -300 , and for case B, it is about $+1600$. Since K_I is positive, one obtained a negative Γ in case A and a positive Γ in case B. Using now the values for Γ and m^* as obtained for case B (assuming U^{4+}) from consideration of ferromagnetic coupling, and the measured value of K_I [Eq. (4)], we find that the hyperfine coupling constant of hydrogen (proton or deuteron) is $A(s) = 1 \times 10^{-6}$ eV $= 9 \times 10^{-3}$ cm $^{-1}$ [if U^{3+} or U^{5+} are assumed, $A(s)$ must be multiplied by 1.03 or 0.735, respectively]. This gives us the electron density at the nucleus $n(0) = u^2(0) = 0.4$ electrons $\text{\AA}^{-3} = 0.175 n_{1s}(0)$, where $n_{1s}(0)$ is the density of the $1s$ hydrogen wave function at the origin.

The calculation of the electron functions in the hydride presents difficulties. Energy-band calculations have not yet been carried out for this compound, and will obviously present difficulties, both due to the presence of uranium ions and because of the complicated crystalline structure of the material. We shall, therefore, attempt an approximate method. Over the years, the chemists have been discussing the problem of structure of metal hydrides, and two theories (models) have come

to the fore^{32,49,50}: One being the "protonic" theory which assumes that the protons enter the lattice, frequently substitutionally, while their electrons enter the conduction band of the metal; the anionic theory assumes, on the contrary, that hydrogen enters the lattice as H^- ions. The stoichiometry of uranium hydride seems to argue against the protonic model; the distances between adjoining pairs of hydrogens exclude the assumption of H_2 units in the lattice. The anionic theory accounts nicely for the uranium-hydrogen distances,⁵⁰ but since such hydrogen would have paired electrons, this model could hardly account for the strong contact interaction observed. Because of the negative charge of the H^- ion, conduction electrons would be repulsed by it, and their density at the proton reduced. Thus, both direct and indirect contact interactions would be greatly reduced.

We, therefore, propose a model based on a suggestion by Gibb,⁴⁹ who tries to reconcile both aspects. It is applied here to UH_3 , and it is not at all clear whether it will be applicable to other metal hydrides. It also does not explain why UH_3 (as different from other hydrides) appears only in its stoichiometric composition. We assume that the lattice is constructed out of uranium ions, which give rise to a conduction band originating out of $6d-7s$ uranium states. This conduction band is rather narrow, with a high electron density $n(E_F)$ at the Fermi level. We now further assume that the conduction electrons can be treated as nearly free and that they are evenly spread over the crystal volume. This may be made plausible by arguments reminiscent of pseudopotential theory, where appropriate calculations smooth out the wave-function fluctuations inside ion cores, and the resulting pseudo-wave-function usually shows comparatively slight departure from free-electron behavior. Whether pseudopotential theory is applicable to UH_3 or to uranium (because of the presence of $5f$ electrons) is beside the point. It has only been argued that, over most of the crystal volume, the conduction electrons can be treated as "free." Hydrogen atoms are now introduced into this lattice. Their electrons enter the conduction band (as in the original protonic theory). However, as the "bare" protons now show a positive charge, free electrons will be attracted and form a negative screening cloud around the proton sites. This picture has been used for 30 years to discuss impurities in metals. Here, we apply it to a stoichiometric lattice. It is assumed that the charges on different hydrogen sites do not interfere appreciably with one another.

The model consists of a lattice of N uranium ions U^{+v} and a single proton H^+ at the origin of the coordinates, in a sea of conduction electrons. At the positive-ion sites, the density of electrons is increased

⁴⁶ K. Yosida, *Phys. Rev.* **106**, 893 (1957); P. G. de Gennes, *J. Phys. Radium* **23**, 510 (1962).

⁴⁷ V. Jaccarino, B. Matthias, M. Peter, H. Suhl, and J. H. Wernick, *Phys. Rev. Letters* **5**, 251 (1960); V. Jaccarino, *J. Appl. Phys.* **32**, 102S (1961); A. C. Gossard, V. Jaccarino, and J. H. Wernick, *Phys. Rev.* **128**, 1038 (1962).

⁴⁸ A. M. van Diepen, H. W. de Wijn, and K. H. J. Buschow, *J. Chem. Phys.* **46**, 3489 (1967); H. W. de Wijn, A. M. van Diepen, and K. H. J. Buschow, *Phys. Rev.* **161**, 253 (1967).

⁴⁹ T. R. P. Gibb, Jr., in *Progress in Inorganic Chemistry*, edited by F. A. Cotton (Wiley-Interscience, Inc., New York, 1962), Vol. 3, pp. 315-509; in *Advances in Chemistry Series* (American Chemical Society, Washington, D. C., 1963), Vol. 39, pp. 99-110.

⁵⁰ G. G. Libowitz, in *Advances in Chemistry Series* (American Chemical Society, Washington, D. C., 1963), Vol. 39, pp. 74-86.

compared with the average density. In order to estimate the distribution of electrons on and around the proton, assume that, in the vicinity of the proton, the conduction electrons can be described by the Hamiltonian

$$\mathcal{H}C = (\hbar^2/2m)\sum_i \nabla_i^2 + \sum_i V(r_i - R_0) + \sum_{i,j \neq 0} V(r_i - R_j) + \sum_{i>j} V(r_i - r_j), \quad (42)$$

where the second term represents the proton-electron interactions, the third is the potential energy of the electrons in the field of all the other ions, and the last represents the electron-electron interaction. In the vicinity of the proton, we neglect the detailed influence of other ions and replace it by an average space-charge density, as in jellium. Referring the electron energy to the constant-background potential of all the ions, we effectively remove the third term of Eq. (42). The remaining Hamiltonian is reminiscent of a point impurity in an interacting electron gas. This can be treated by several methods.

(a) the Thomas-Fermi approach, as used originally by Mott,⁵¹ is unsuitable for our purpose, since electron density tends to infinity for $r \rightarrow 0$.

(b) The pseudopotential methods or Friedel's scattering model⁵² are also unsuitable, as they obtain correctly the behavior of electrons outside the given ion core, but inside they replace it by a simplified model. However, this is the region in which we are primarily interested.

(c) The Hartree-Fock self-consistent approach calculations, as carried out by March and Murray⁵³ and others, has been used.

(d) Langer and Vosko⁵⁴ attacked the problem using many-body theory methods. All approaches indicate appreciable heaping up of electrons around the positive impurity.

In order to calculate the Knight shift, one requires to know $n(0)$, the electron density at the proton. We assume that there is a uniform electron density $n_0 = 8Z/V_c$, where Z is the number of conduction electrons per uranium ion which contribute to n_0 , and V_c is the crystal cell volume which contains eight uranium atoms. We obtain the excess electron density of the proton from March and Murray's⁵³ and from Langer and Vosko's⁵⁴ calculations (Fig. 14). Figure 14 shows the relative excess density at the origin $\Delta n(0)/n_0$ as a function of r_s , where r_s is the radius (in units of the Bohr radius a_0) of a sphere which contains one electron

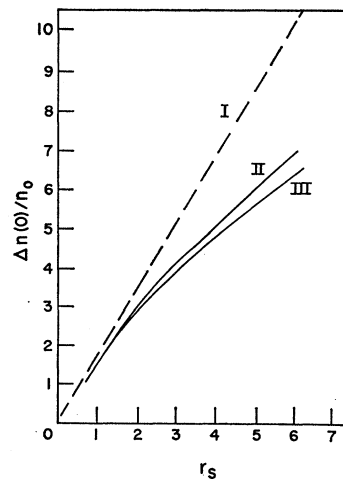


FIG. 14. The calculated relative excess electron concentration at the proton $\Delta n(0)/n_0$ as a function of r_s , the radius of a sphere which contains one electron at average density n_0 . (I) was derived by March and Murray (see Ref. 53); (II) and (III) are from Langer and Vosko (see Ref. 54).

$n_0 = [(4\pi/3)(r_s a_0)^3]^{-1} e \text{ \AA}^{-3}$. The calculations agree well, though March and Murray's⁵³ give slightly higher values for low n_0 . We calculated $n(0) = n_0[1 + \Delta n(0)/n_0]$ for several values of n_0 . For case B, ($Z=2.5$), we obtained $n_0 = 0.069 e \text{ \AA}^{-3}$ and $n(0) = 0.34 e \text{ \AA}^{-3}$, which agrees well with the value $0.4 e \text{ \AA}^{-3}$ obtained above from the experimentally measured Knight shift and assumed RKKY coupling. The value of $n(0)$ is not very sensitive to the choice of n_0 , since a change in n_0 is partially compensated by an opposite change in $\Delta n(0)/n_0$.

Libowitz⁵⁰ derived the "radius" of the H^- ion in uranium hydride from considerations of ionic radii in metal hydrides and obtained $r_H = 1.27 \text{ \AA}$. This value accounts for the U-H distances in $\beta\text{-UH}_3$. However, the radius deduced from the shortest H-H distance in $\beta\text{-UH}_3$ is slightly lower. Assuming $r_H = 1.27 \text{ \AA}$, we calculated the additional screening charge q' around the proton by numerical integration of $\Delta n(r)$, using tabulations by Langer and Vosko,⁵⁴ and we obtained, for case B, the value $q' = 0.8$ electrons.

The total charge within $r_H = 1.27 \text{ \AA}$, including the contribution of the average conduction-electrons density ($\frac{4}{3}\pi r_H^3 n_0 = 0.6 e$), is now $1.4 e$. The result is sensitive to the radius assumed for the hydrogen ion and to the average electron density. Z , the number of conduction electrons per UH_3 , and the sum of the excess charge on the three hydrogens should equal the total number of electrons provided by three hydrogens and one uranium ion, thus determining the valency v of the latter. In case B, $Z=2.5$, and the electron accumulation around the three hydrogens is $0.8 \times 3 = 2.4$. Out of 4.9 electrons, three electrons are contributed by the hydrogens, so that $v \sim 1.9$ electrons, implying U^{2+} , while, for example, for $Z \sim 3.5$, one obtains $v \sim 3$. However, since the calculations are very sensitive to the parameters chosen and

⁵¹ N. F. Mott and H. Jones, *Metals and Alloys* (Clarendon Press, Oxford, 1936); H. Schnabel, *Ber. Bunsenger* **68**, 549 (1964).

⁵² J. Friedel, *Advan. Phys.* **3**, 446 (1954); E. Daniel, *J. Phys. Radium* **20**, 769 (1959); **20**, 849 (1959).

⁵³ N. H. March and A. M. Murray, *Proc. Roy. Soc. (London)* **A256**, 400 (1960); **A260**, 119 (1961); **A266**, 559 (1962).

⁵⁴ J. S. Langer and S. H. Vosko, *J. Phys. Chem. Solids* **12**, 196 (1959).

we have neglected the fact that there is also an excess charge of conduction electrons around the positive uranium ions, the result should be viewed with suspicion.

VIII. QUADRUPOLE COUPLING

Quadrupole coupling constants of deuterons have been measured in a number of compounds and have been reviewed recently by Pyykkö.⁵⁵ The couplings are of the order of 100–300 kHz. The Sternheimer's anti-shielding factors for isolated H and H^- are of the order of 1, but of opposite sign. Uranium hydride is metallic and the calculations of electric field gradients in metals⁵⁶ are more difficult than in, e.g., ionic compounds. The problem has been discussed at length by Watson *et al.*⁵⁷ They consider electric field gradients in metals as resulting from two distinct effects: from the ions in the lattice, external to the ion considered, which contribute q_{latt} , and from electrons within the ionic sphere of the nucleus considered. The latter contribution is analyzed in terms of three contributions as follows:

(1) q° , which is due to Bloch electrons within the ionic sphere. Since in $\beta\text{-UH}_3$ at the H sites, the point symmetry is approximately tetrahedral (the four adjoining uranium ions are arranged in a nearly perfect tetrahedron), the local symmetry of the Bloch electrons must be of similar symmetry and, hence, its contribution must vanish. This is not strictly correct, since we have neglected the neighboring H ions, which spoil the symmetry.

(2) q' , which is due to redistribution of conduction electrons around E_F , the Fermi energy, since, because of the q_{latt} terms in the potential, their eigenvalues are

slightly shifted, and this will cause redistribution of electrons among the eigenstates. This effect is important if $n(E_F)$ is high (which is the case in uranium hydride).

(3) q'' , which is associated with the fact that all wave functions are perturbed by q_{latt} and, thus, excited states are admixed. This is true for electrons of all energies and not only for those in the vicinity of the Fermi surface.

We calculated q_{latt} using lattice sums for different combinations of point charges on the U and H sites (Fig. 15) and checked the convergence of the summations. The q_{latt} is not very sensitive to the variations of charges on the hydrogen sites.

In order to assess the effect of conduction electrons, we used a variation of the Thomas-Fermi approximation.⁵⁸ Let the energy of the electrons around the hydrogen be given by

$$p^2/2m^* - eV(r) - (\frac{1}{2}e^2)q_{\text{latt}}P_2^0(\theta, \phi)r^2 = 0, \quad (43)$$

where V is the unperturbed potential, as derived in a self-consistent manner, e.g., from Thomas-Fermi function. Then, owing to the presence of the perturbation term q_{latt} , the change in charge distribution is given by

$$\Delta n(r, \theta, \phi) = -2\pi^{2/3}h^{-3}m^*e^2q_{\text{latt}}P_2^0r^2n^{1/3}(r), \quad (44)$$

where $n(r)$ is the undisturbed electron distribution. Thus,

$$\Delta q/q_{\text{latt}} = -2(5\pi^{1/3}a_0)^{-1}(m)/m_e \int_0^{r_H} n^{1/3}(r)rdr. \quad (45)$$

We evaluated the integral using tabulations of Langer and Vosko,⁵⁴ which are preferable to the Thomas-Fermi functions used originally by Sternheimer.⁵⁸ The result is again sensitive to the choice of radius k_F and effective mass. For case B, $m^*/m_e = 3$, we obtained $\Delta q/q_{\text{latt}} = -0.65$.

The above calculation is equivalent to evaluation of q' in the terminology of Watson *et al.*⁵⁷ The Thomas-Fermi model populates all states up to E_F by filling the momentum space at constant density. In the case of spherically symmetric potential, the occupied space is a sphere. Under the influence of q_{latt} , it becomes distorted, but this affects only the occupation of states near the Fermi surface.

We suspect that uranium ions are present as U^{4+} . Together with the calculated excess charge of $\sim 0.8e$ on the hydrogen sites, this gives $e^2q_{\text{latt}}Q/h = 36$ kHz and $\eta = 0.23$. If the shielding of the conduction electrons is also considered, one obtains $e^2qQ/h = 11.3$ kHz, which is close to the experimental result. However, as the parameters used are based on a number of assumptions of doubtful validity, it is not clear what reliability one can attach to the numerical results. It can be concluded that, although the assumption of U^{4+} ions seems to be compatible with the calculations, the presence of U^{3+} ,

⁵⁸ R. M. Sternheimer, Phys. Rev. **80**, 102 (1950); **96**, 966(E) (1954).

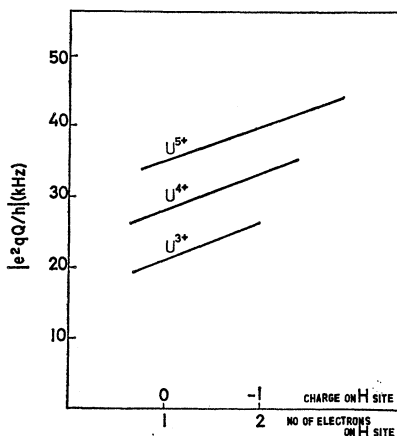


FIG. 15. The calculated deuteron quadrupole interaction $|e^2qQ/h|$ (on the assumption of n_0 shielding) as a function of the charge on the hydrogen sites.

⁵⁵ P. Pyykkö, Ann. Univ. Turku, Ser. A, No. **103** (1967).

⁵⁶ A. Weiss, *Magnetic Resonance and Relaxation—XIVth Colloque Ampère, Ljubljana, 1966* (North-Holland Publishing Co., Amsterdam, 1967), p. 1076.

⁵⁷ R. E. Watson, A. C. Gossard, and Y. Yafet, Phys. Rev. **140**, A375 (1965).

U^{5+} , or even U^{2+} cannot be definitely excluded on the basis of the measured quadrupole coupling.

IX. SUMMARY

We have attempted to account for some properties of uranium hydride, using a model which assumes that the compound consists of uranium ions and protons (deuterons) in a high-density interacting electron gas and that the magnetic moments arise from localized $5f$ electrons. The uranium ions are assumed to be magnetically coupled through the conduction electrons (RKKY-type coupling), which accounts for the ferromagnetic ordering below 180°K . From this, we conclude that there are about $Z \sim 2.5$ conduction electrons per uranium atom and that the interaction constant is $\Gamma \sim 20 \text{ eV } \text{\AA}^3$ and $m^*/m_e \sim 3$. Contact interaction between the nuclei and the polarized conduction electrons at the hydrogen site accounts for the observed Knight shift, which is the same for both isotopes and proportional to the susceptibility: $K = (0.40 \pm 0.03)\chi_M$. This large shift is due to polarization of conduction electrons via the RKKY interaction and is magnified by the high concentration of electrons at the nucleus.

Measurements of the second moment of the hydride confirmed the second structure proposed by Rundle⁸ (while the originally proposed structure^{8,19} would require an internuclear second moment $M_V = 40 \text{ Oe}^2$, which is much higher than the observed $M_V = 24 \pm 2 \text{ Oe}^2$). Second moment and line-shape measurements confirmed that the $5f$ electrons are localized and do not form a band (as in metallic uranium). The experimental line shapes were compared with lines calculated on the assumption of three line-broadening mechanisms (apart from the quadrupolar interaction in the deuteride), namely, internuclear broadening, the (classical) dipole fields of paramagnetic ions, and the effect of powder structure. It has been shown that only a particular combination of line-broadening parameters reproduce the observed line shape (and second moment).

The quadrupole interaction in the deuteride has been determined as $|e^2Qq/h| = 14.5 \pm 0.5 \text{ kHz}$, and results using the calculated antishielding factor seem to point to the presence of uranium as U^{4+} ions, although this conclusion is not definite. Consideration of the magnetic saturation moment in the ordered state and of the susceptibility in the paramagnetic state, also, did not allow a decision in the matter. Thus, the presence of uranium as U^{5+} , U^{3+} , or U^{2+} ions cannot be definitely excluded. NMR lines in uranium hydride narrow at high temperatures ($> 370^\circ\text{K}$). This is due to hydrogen diffusion with an activation energy of $E = 8.4 \pm 0.9 \text{ kcal/mole}$ in $\beta\text{-UH}_3$ and $8.9 \pm 0.9 \text{ kcal/mole}$ in $\beta\text{-UD}_3$ which is the same for both isotopes within the limits of the error. The diffusion takes place by a vacancy

mechanism. It would be of interest to carry out diffusion measurements under varying pressures of hydrogen, especially at high pressures, where the vacancy concentration could be reduced and, thus, our model for diffusion checked.

APPENDIX

In a powder sample, the nucleus experiences the following contributions to the external field H_0 ¹⁸:

(a) A dipolar field arising from the neighboring nuclei in the same particle. This field contributes to the line broadening, but it causes no shift of the resonance line.

(b) A Lorentz field from a spherical surface drawn around the nucleus within its own powder grain, given by $H' = \frac{4}{3}\pi\chi_V H_0$, where χ_V is the volume susceptibility of the solid.

(c) A demagnetization field arising from the grain surface $H'' = -4\pi N_p \chi_V H_0$, where N_p is the demagnetization factor of the powder grain in the direction of the external field.

(d) A Lorentz field arising from a spherical surface around the nucleus, containing many grains in the powder sample $H''' = \frac{4}{3}\pi\chi_V' H_0$, where χ_V' is the volume susceptibility of the powder sample.

(e) A demagnetization field arising from the sample surface $H'''' = -4\pi N_p' \chi_V' H_0$, N_p' being the demagnetization factor of the sample in the direction of the external field. We consider here the powder sample as a continuum with the density of the powder.

The total shift due to the above effects is

$$\delta H^* = 4\pi\left(\frac{1}{3} - N_p\right)\chi_V H_0 + 4\pi\left(\frac{1}{3} - N_p'\right)\chi_V' H_0. \quad (\text{A1})$$

These fields also cause broadening of the NMR line (Drain effect). In this expression, the first term vanishes on averaging, assuming that the particles in the powder are randomly oriented, so that $\bar{N}_p = \frac{1}{3}$. The second term vanishes only if the sample is spherical. Our samples closely approximated the shape of an ellipsoid of axial ratio $m = 5$, with the magnetic field perpendicular to the long axis; thus,

$$N_p' \sim N_{11}(m=5) = \frac{1}{2}[1 - N_{11}(m=5)] = 0.472. \quad (\text{A2})$$

Using this value in Eq. (A1), one obtains

$$K^* = \delta H^*/H_0 = -4\pi \times 0.139\chi_V' = -1.75\chi_V'. \quad (\text{A3})$$

As the sample density is about one-third of the particle density (11 g/cm^3), $\chi_V'/\chi_M = \frac{1}{3}(11/241) = 0.0152$, so

$$K^* \sim -0.025\chi_M. \quad (\text{A4})$$

This shift is negative, toward a lower field at the nucleus. Since the measured shift is positive, we obtain for the corrected Knight shift K_r

$$K_r = K - K^*. \quad (\text{A5})$$

¹⁸ L. Pauling and F. J. Ewing, J. Am. Chem. Soc. **70**, 1660 (1948).